STRUCTURE/ACTIVITY RELATIONSHIP OF α-CONOTOXINS TARGETING $GABA_B$ RECEPTOR

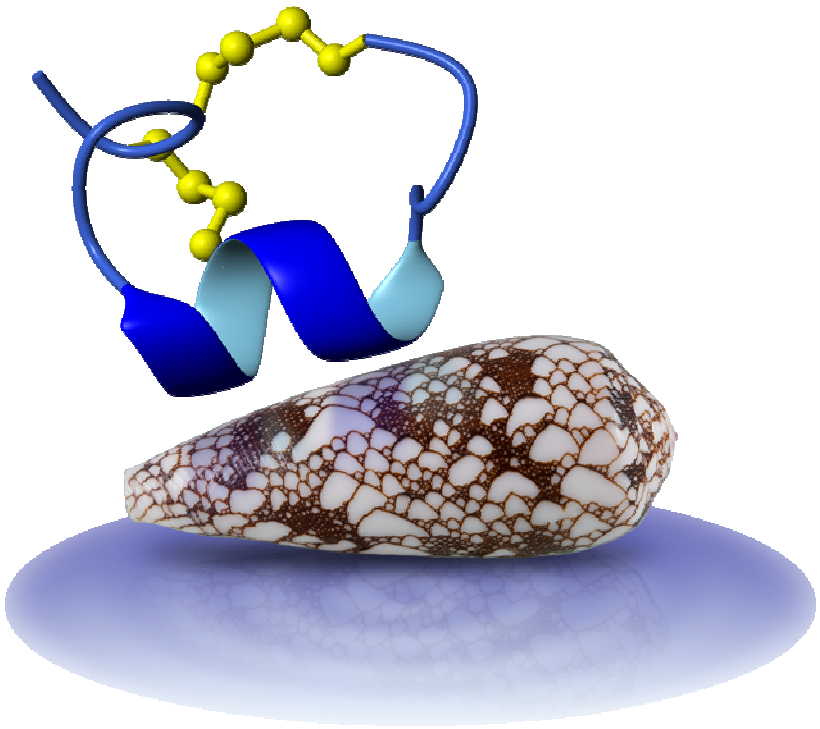

Katrine Sperstad Køller

Institute for Molecular Bioscience

The University of Queensland

Institutt for Farmasi

Universitetet i Tromsø

May 2011

Abstract

Conotoxins are small disulfide rich peptides derived from the venom of Cone snails. They target different receptors in the nervous system with high selectivity and potency making them valuable as drug leads or drug themselves. One group of conotoxins, α-conotoxins have been shown to have potential as treatment for neuropathic pain.

α-conotoxins share a number of conserved structural features. They contain two disulfide bonds between Cys^{I}-Cys^{III} and Cys^{II}-Cys^{IV} and an α-helix spanning around Cys^{III} making them form two loops in their backbone. The aim of my thesis was to examine the structure/activity relationship of α-conotoxins inhibiting N-type Ca^{2+} channels via $GABA_B$ receptor by swapping the loops between Vc1.1, PeIA, AuIB and RgIA.

Four chimeric conotoxins were synthesised and NMR spectroscopy was used to confirm that they maintained the characteristic overall fold as the native α-conotoxins and bioactivity assays were performed to see if the activity was changed.

Although the structural characteristics of all four chimeric α-conotoxins were similar to the native peptide, their ability to inhibit N-type Ca^{2+} channel currents by $GABA_B$ receptor activation was reduced compared to the native conotoxins. The loss of activity observed between these peptides suggests that there is two loops function cooperatively to interact with the $GABA_B$ receptor. This study provides preliminary structure/activity data that will form the basis of future work towards the design and synthesis of more potent and selective conotoxin analogues as drug leads for the treament of pain.

Acknowledgements

This project was performed at Institute of Molecular Bioscience at the University of Queensland, Australia, in the period from October 2010 to May 2011.

First I wish to say thank you to my supervisor Dr. Richard Clark for his guidance and support throughout the study and helpful comments on writing my master thesis. Especially I want to thank you for how you always took the time to answer my questions or help me with the equipment in the lab, regardless of how busy you were, which is very much appreciated.

I would like to express my gratitude to Professor David Craik for having me as a master student in his lab, and to Dr. Johan Rosengren for helping me with NMR structure analysis.

Furthermore I would like to thank all members of the Craik group for helping me in the lab, especially Chia Chia Tan for showing me how to use the different analytical instruments. You all made my stay here enjoyable.

A would like to express thanks to Iselin for sharing this experience with me and to my friends, especially Rob Ling, for all the support throughout this year.

Finally I would like to thank Dr. Jon Våbenø at The University of Tromsø for being my internal supervisor and giving me the opportunity to do my thesis in Australia.

List of Abbrevations

BOC	t-butoxycarbonyl
CNS	Central nervous system
DIPEA	diisopropylethylamine
DMF	dimethylformamide
ECOSY	Exclusive correlation spectrometry
ES-MS	Electrospray mass spectrometry
FMOC	9-fluorenylmethyloxycarbonyl
GABA	γ-amino-butyric acid
GPCR	G-protein coupled receptor
HBTU	O-benzotriazol-1-yl-1,1,3,3-tetramethyluronium hexafluorophosphate
HF	Hydrofluoric acid
HPLC	high performance liquid chromatography
MALDI-MS	Matrix assisted Laser Desorption Ionisation Mass Spectrometry
nAChR	Nicotinic acetylcholine receptor
NMR	Nuclear magnetic resonance
NOE	Nuclear Overhauser effect
NOESY	Nuclear Overhauser Enhancement Spectroscopy
RMSD	Root mean square deviation
RP-HPLC	Reverse phase high performance liquid chromatography
SPPS	Solid phase peptide synthesis
TFA	Trifluoroacetic acid
TOCSY	Total Correlation Spectroscopy
Å	Ångström

Table of content

1 Introduction **9**

1.1 Cone snails *9*

1.2 Conotoxins *10*

1.2.1 Conotoxin classification and nomenclature **11**

1.2.2 Therapeutics application of conotoxins **12**

1.3 α-conotoxins *12*

1.3.1 Structure **12**

1.3.2 Activity **14**

1.4 α-conotoxins targeting the $GABA_B$ receptor. *14*

1.5 $GABA_B$ receptor *15*

1.6 Neuropathic pain *16*

1.7 Aim of my project *17*

1.8 Solid Phase Peptide Synthesis *18*

2 Results **20**

2.1 Peptide synthesis *20*

2.2 Peptide folding *21*

2.3 NMR *22*

2.3.1 Assignment of Spectra **22**

2.3.2 Structural assignment **26**

2.4 Bioactivity ***30***

3 Discussion **32**

4 Conclusion **37**

5 Material and methods **38**

5.1 Peptide synthesis ***38***

5.2 Peptide folding ***39***

5.3 NMR spectroscopy ***40***

5.3.1 Spectral assignment **40**

5.3.2 Structural assignment **40**

5.4 Determining the concentration of a peptide solution ***41***

5.5 Bioactivity ***41***

5.6 Analytical instruments ***42***

5.6.1 Preparative and Semipreparative HPLC **42**

5.6.2 Analytical HPLC **42**

5.6.3 Mass spectrometry **43**

6 Appendix **44**

7 References **47**

1 Introduction

1.1 Cone snails

Cone snails (Genus *Conus*) are venomous predatory gastropods that live in tropical and subtropical seas [1] Their beautiful patterned shell has been admired by collectors for centuries [2] (see Fig. 1) , but it was their interactions with human that has captivated scientists. They observed a number of patients presenting numbness when exposed to snail stings [3, 4]. Further studies revealed that the venom produced by Cone snails immobilize and killed their prey [5] by targeting the nervous system [6]. Today ~700 different species in the Conus genus have been described [1]. They are found in a range of different habitats and feed on a variety of prey, like fish, worms and molluscs [1]. Cone snails are slow moving and in order to catch their fast moving prey they have developed an effective strategy. They produce a complex venom cocktail consisting of highly potent and selective peptides that act synergistically to quickly numb the prey [7]. Due to their different habitats and different types of prey they have evolved different venom mixtures and each snail harbors up to 200 different venom peptide components known as conopeptides [8].

Figure 1. *Conus victoriae*.

The conopeptides can be divided into two main groups, the disulfide rich and the disulfide poor (Figure 2). The disulfide poor group contains one or no disulfide bonds, whereas the disulfide rich have two or more disulfide bonds [2, 8]. The disulfide rich conopeptides are called conotoxins and it is this group that is most interesting as therapeutics [1].

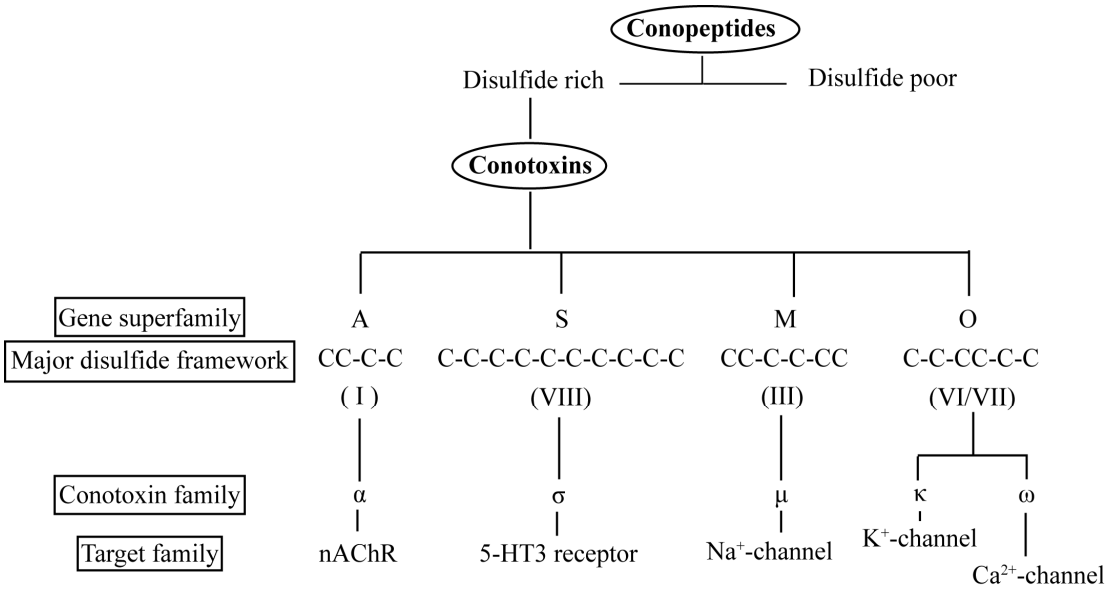

Figure 2. Classification of conopeptides. The disulfide rich group of conopeptides is called conotoxins, and they are divided into gene superfamilies according to the signal sequence of the conotoxin precursor. They are further classified according to their disulfide framework given a roman number and their pharmacological target given a greek letter.

1.2 Conotoxins

Conotoxins are the largest group of conopeptides. They are small in size, typically 12-30 amino acids, but because of the disulfide bridges they are very stable in their conformation compared to other small peptides [7]. They have been found to target different membrane receptors such as nicotinic acetylcholine receptors (nAChR) and ion channels such as K^+- and Na^+- channels with high selectivity [1, 8]. Their ability to target

different receptors in the nervous system with a high potency and selectivity makes them a valuable neuropharmacological resource [9].

1.2.1 Conotoxin classification and nomenclature

Conotoxins are classified in three steps according to their characteristics (Figure 2) [10]. They are divided into superfamilies based on the signal sequence of the conotoxin precursors, with each superfamily designated by an uppercase letter [1, 11]. Then they are classified according to their disulfide framework, indicated by a roman number. Some superfamilies can have more than one set of frameworks, like the O – superfamily as shown in Figure 2. They are further divided into conotoxin families according to their pharmacological activity, each target given a greek letter. For example μ-conotoxin family members are Na^+ channel blocker.

When naming an individual conotoxin, the greek letter signifying the conotoxin family comes first (Figure 3). Then one or two they letters indicate which conus species the peptide is derived from, for example Rg for the *Conus regius*. After that comes a Roman number representing their cysteine framework. Typically at the end an upper case letter is added in order of discovery [1].

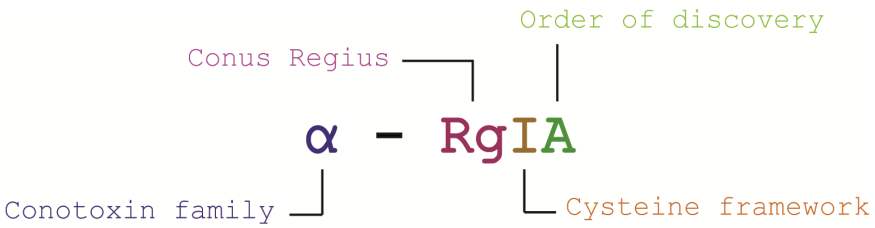

Figure 3. Conotoxin nomenclature. The structure of naming conotoxins begins with the greek letter representing the conotoxin family and target followed by one or two letters indicating which species the peptide is derived from. Then comes a roman letter showing the cysteine framework and in most peptides an upper case letter is given at the end according to the order of discovery.

1.2.2 Therapeutics application of conotoxins

Conotoxins have evolved to target a wide range of targets, and with their structural stability, potency and specificity they are invaluable as new drug leads and for detecting new pharmacological mechanisms [1, 11]

Many of the pharmacological targets of conotoxins are associated with pain pathways [12], and new drug targets for severe pain have been discovered through research on conotoxins [11]. 10 % of the first 30 characterized peptides from Conus venoms have reached clinical trials where pain is the major indication [11]. One ω-conotoxin, ω-MVIIA (Ziconitide), an antagonist of N-type calcium channels and has been approved by the US Food and Drug Administration (FDA) in 2004 and by European Medicines Agency (EMEA) in 2005 for intrathecal treatment of severe chronic pain [13].

1.3 α-conotoxins

1.3.1 Structure

α-conotoxins were the first conotoxins discovered [14] ranging from 12-19 amino acids in length. They are defined as being competitive antagonists of nicotinic acetylcholine receptors [15] and share a number of conserved structural features. They typically have an amidated C-terminus and they all follow the same cysteine pattern, CC-C-C, defined as framework I.

The four cystines form two disulfide bridges in three different ways (Figure 4), globular, ribbon and beads but the majority of the α-conotoxins form the globular connectivity in their native structures [15]. The disulfide bridges make the peptide form two loops in their backbone (Figure 5). The number of residues within these loops varies among the different α-conotoxins and these spacings are used to divide the α-conotoxins into

subclasses (Table 1). For example RgIA has 4 residues in the first loop and 3 residues in the second loop and thereby is a member of the 4/3 subclass.

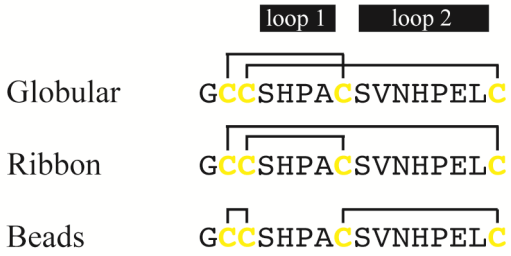

Figure 4. Disulfide connectivity. α-conotoxins form three different disulfide connectivities, Globular, Ribbon and Beads, with the majority forming globular. The residues between the cysteines form two loops indicated by the black boxes.

Nuclear magnetic resonance (NMR) spectroscopy and x-ray crystallography have been used to determine the three dimensional structure of conotoxins [16, 17]. NMR spectroscopy is the predominant method for determining the structure of disulfide rich peptides and is particularly suited to conotoxins, which are are relatively small in size and difficult to crystallize due to their high aqueous solubility. α-conotoxins have a common three dimensional structural topology (Figure 5). The cross bracing provided by the two disulfide bridges gives them a well defined structure that is both relatively stable and rigid. α-conotoxins typically forms an α-helix that is centered around Cys^{III}.

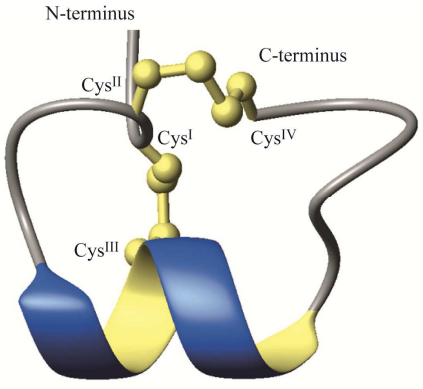

Figure 5. Three dimensional structure of α-conotoxin Vc1.1 showing the α-helix spanning around Cys^{III} and globular disulfide connectivity.

1.3.2 Activity

α-conotoxins target nAChR, both neuronal and muscle type, where they act as antagonists. The nAChR consist of five homologous subunits, α, β, δ and γ [18] and different combination of these subunits gives rise to different subtypes of nAChR [18]. α-conotoxins show varying degrees of selectivity for the different subtypes of nAChRs fig such as α3β2, α3β4, α7, α9α10. Recently another novel molecular target for α-conotoxins was reported, the inhibition of voltage dependant N-type calcium channels via $GABA_B$ receptor activation [12].

1.4 α-conotoxins targeting the $GABA_B$ receptor.

Structure/activity and electrophysiological studies have revealed that α-conotoxins Vc1.1 and RgIA inhibit high voltage activated N – type ($Ca_v2.2$) calcium channel currents in rat dorsal ganglia root neurons via $GABA_B$ receptor activation [12]. This mechanism is likely to produce the anti allodynia effects of Vc1.1 and RgIA [12, 19]. Two other α-conotoxins AuIB [19] and PeIA [20] have recently been reported to also inhibit N-type calcium channels by acting as agonists via G-protein-coupled $GABA_B$ receptors. The sequences of these four peptides are shown in Table 1.

Table 1. Sequences of α – conotoxins targeting the $GABA_B$ receptor. The table also shows the different subclasses to the peptides, which α-conotoxins are divided into according to the number of residues within their loops.

Name	Sequence	Subclass
PeIA	G**CC**SHPA**C**SVNHPEL**C**	4/7
Vc1.1	G**CC**SDPR**C**NYDHPEI**C**	4/7
RgIA	G**CC**SDPR**C**RYR**C**	4/3
AuIB	G**CC**SYPP**C**FATNPD**C**	4/6

1.5 $GABA_B$ receptor

The $GABA_B$ receptor is the target for the major inhibitory neurotransmitter in the central nervous system (CNS), γ-amino-butyric acid (GABA) [21, 22]. GABA targets both the $GABA_A$ receptor, which is an ion channel receptor, and the $GABA_B$ receptor, which is a G-protein coupled receptor (GPCR) [21]. Characterization of the $GABA_B$ receptor at a molecular level was only recently determined [23-28] and it was the first GPCR discovered to be a heterodimer.

The $GABA_B$ receptor consists of two seven-transmembrane domains. The G-protein binds intracellular to the transmembrane domains (Figure 6) consisting of 3 subunits, α, β and γ, with β and γ forming a complex. In an inactivated state α and βγ are together but when a ligand binds to the receptor they get activated and separate from each other (Figure 7). After separation they bind to other receptor targets such as ion channels for example voltage dependant N – or P/Q type Ca^{2+}-channels and K^+-channels or/and second messengers for example adenylyl cyclase [21, 22, 29].
$GABA_B$ receptor agonists are found to be involved in nociception, drug and alcohol addiction and gastroesophageal reflux diseases [21, 30-35] whereas $GABA_B$ receptor antagonists have potential as antidepressants and in treating cognitive impairment [36-38]. Baclofen is the only selective $GABA_B$ agonist [39] on the market today. It was introduced in 1972 and is prescribed as an antispastic agent and muscle relaxant [40].

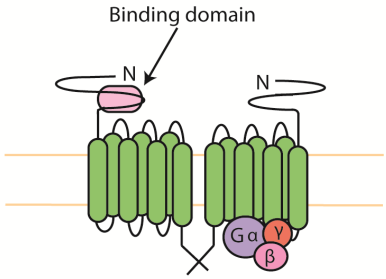

Figure 6. The structure of G-protein coupled $GABA_B$ receptor. The receptor consists of a heterodimer of two seven-transmembran domains with the N-terminus extracellular and the C-terminus intracellular. The binding domain to which the ligand binds is localized extracellular. The G-protein subunits α, β and γ is bound to the receptor intracellular.

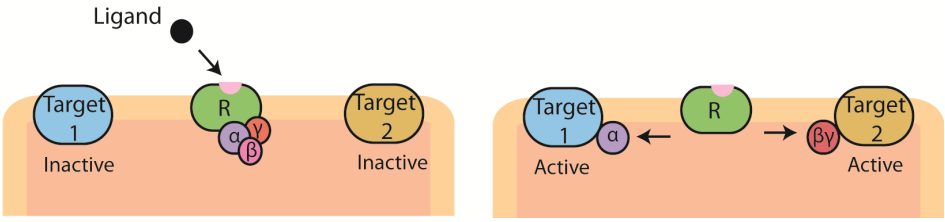

Figure 7. The activation/function of the G-protein coupled receptor. a) A ligand binds the receptor and the G-protein gets activated. b) β and γ forms a complex and both α and the βγ-complex, or just one of them dissociate from the receptor and activate the target.

1.6 Neuropathic pain

According to NeuPSIG (Special Interest Group on Neuropathic pain) neuropathic pain is defined as "pain arising as a direct consequence of a lesion or disease affecting the somatosensory system" [41]. The prevalence of neuropathic pain is been estimated to affect 7-8 % of the population in Europe [42, 43]. It can be caused by different diseases like diabetic peripheral neuropathy, herpes zoster, multiple sclerosis, stroke, spinal cord injury and amputations [44, 45]. The mechanism is complex and involves both the peripheral and central nervous system resulting in hyperexitable sensitization of the neurons [46, 47]. Neuropathic pain reduces the quality of life of the people affected and it is a substantial cost to society [47, 48]. Recommended first line treatment for neuropathic pain are antidepressants and anticonvulsants while opioids are the second line choice [49]. The drug treatments available to this date is not satisfactory [50]. Many patients suffer from inadequate pain relief due to adverse drug effects, development of tolerance or lack of effect [51] There is a need for new, safer and more potent drugs [52]

1.7 Aim of my project

In this project I want to examine the structure/activity relationship of the α-conotoxins targeting $GABA_B$ receptor. This will be achieved by swapping the loops between these four α-conotoxins to see what effect this will have on their activity and structure. I will make four chimeric peptides (Table 2) and an additional three chimeras have been made by Ms. Chia Chia Tan, which I will structurally characterise. All seven peptides will be tested for their ability to inhibit N-type Ca^{2+} channel currents via the $GABA_B$ receptor.

Table 2. Sequences of the α-conotoxins with swapped loops

Conotoxin	Sequence
PeIA/Vc1.1	G**CC**SHPA**C**NYDHPEI**C**
PeIA/RgIA	G**CC**SHPA**C**RYR**C**
PeIA/AuIB	G**CC**SHPA**C**FATNPD**C**
AuIB/PeIA	G**CC**SYPP**C**SVNHPEL**C**

This specific aims of my project are:

1. To chemically synthesise a series of chimeric conotoxins designed from peptides from different conotoxin sub-families.

2. To structurally characterise the chimeric contotoxins using NMR spectroscopy

3. To assess the biological activity of the chimeric conotoxins to reveal information on the structure/activity relationships of the conotoxins at the $GABA_B$ receptor.

1.8 Solid Phase Peptide Synthesis

All the peptides described in this project were synthesised by solid phase peptide synthesis (SPPS). SPPS was developed by R. B. Merrifield and has become the most common methodology for synthesizing peptides [53] The principle of SPPS, illustrated in Figure 7, is to build up a peptide chain on a solid support consisting of resin beads. The resin is laid on a sintered glass filter in a reaction vessel. In the bottom of the reaction vessels is a tap that is connected to a vacuum line via a solvent trap. This tap is used to drain away the reagents while the resin is retained in the vessel because of the filter.

The main advantages of using solid phase for peptide synthesis are that the reactions can be driven to completion by addition of excess reagents and these reagents can be/is easily removed by washing the resin with an appropriate solvent. Additionally physical loss of the peptide is reduced as it is attached to the solid support during chain assembly.

There are two types of chemistry used in SPPS, t-butoxycarbonyl (BOC) and 9-fluorenylmethyloxycarbonyl (FMOC). The difference between them are the types of reagents for the deprotection step and the reagents used for cleavage. BOC chemistry uses acid (typically Trifluoroacetic acid (TFA)) for deprotection step and requires hydrogen fluoride (HF) for cleavage, while FMOC chemistry utilizes base (typically piperidine) for the deprotection step and TFA for cleavage (which is easier and safer then HF)

The peptides are synthesized from C-terminus to the N-terminus, backwards of how we normally write a sequence. Synthesizing peptides is a repeated cycle of deprotection (Figure 8). The N-terminus containing a protection group (either FMOC or BOC) is deprotected and the activated amino acid is added and allowed to couple. Then follows a new deprotection and the chain is ready for the next amino acid. This continues until all the amino acids are added and the peptide chain is complete.

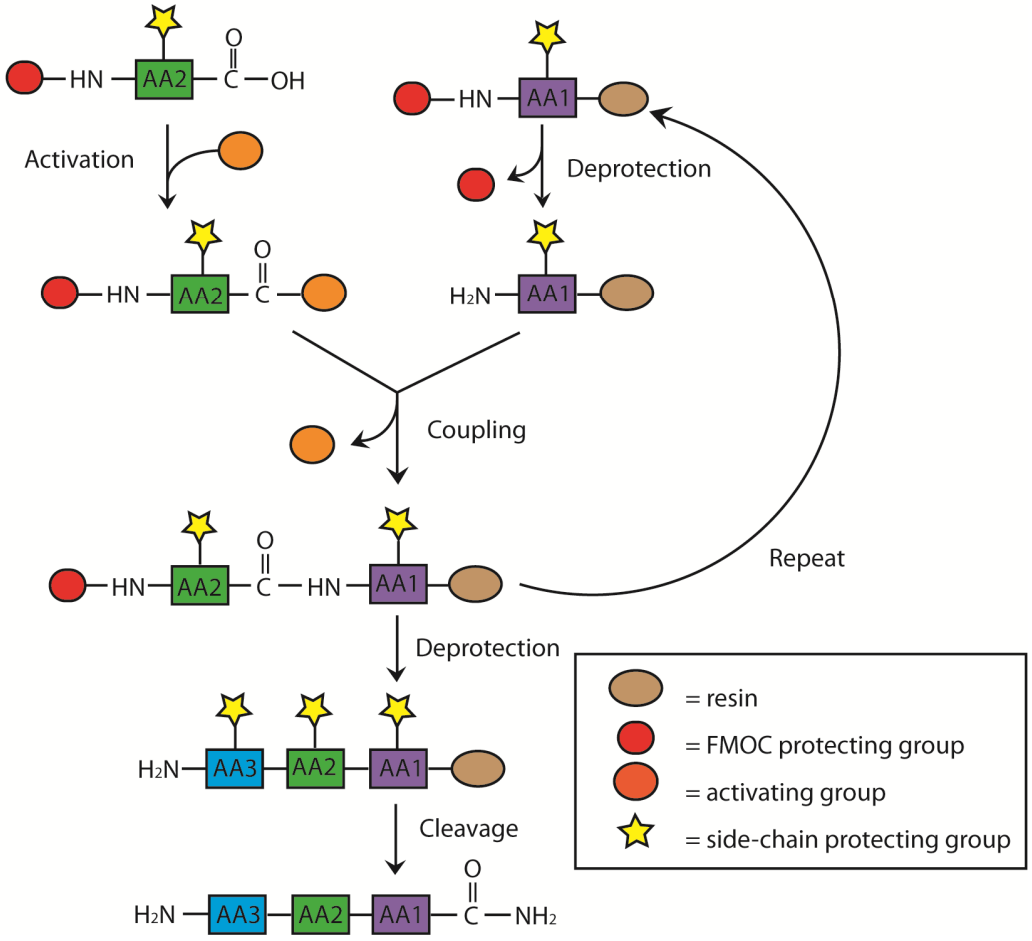

Figure 8. The general principle of solid phase peptide synthesis. The peptide chain is built up upon a resin bead. N-protected amino acids are added to the chain with the aid of an activating agent. The protecting group is then removed to generate the free amino group ready for coupling of the next amino acid in the sequence. This process is repeated until the peptide chain is complete when it is then cleaved from the solid support.

2 Results

2.1 Peptide synthesis

All four chimeric peptides were successfully assembled by solid phase peptide synthesis with FMOC chemistry, the average coupling yield for all peptides was 99.4 – 99.6 %.

The peptides were cleaved from the resin using TFA, and mass spectrometry of the cleaved mixture revealed a major product for each cleavage mixture corresponding to the mass of the desired peptide. The molecular masses of all peptides are shown in table 3. ES-MS spectrum is shown in figure 9, A1,A2 and A3.

Table 3. Molecular weight (g/mol) of the reduced, partly oxidised and fully oxidised chimeric α-conotoxins.

Peptide	M_W reduced	M_W partly oxidised	M_W fully oxidized
PeIA/Vc1.1	1889.9	1887.9	1745.9
PeIA/RgIA	1496.5	1494.5	1352.5
PeIA/AuIB	1666.7	1664.7	1522.7
AuIB/PeIA	1849.9	1847.9	1705.9

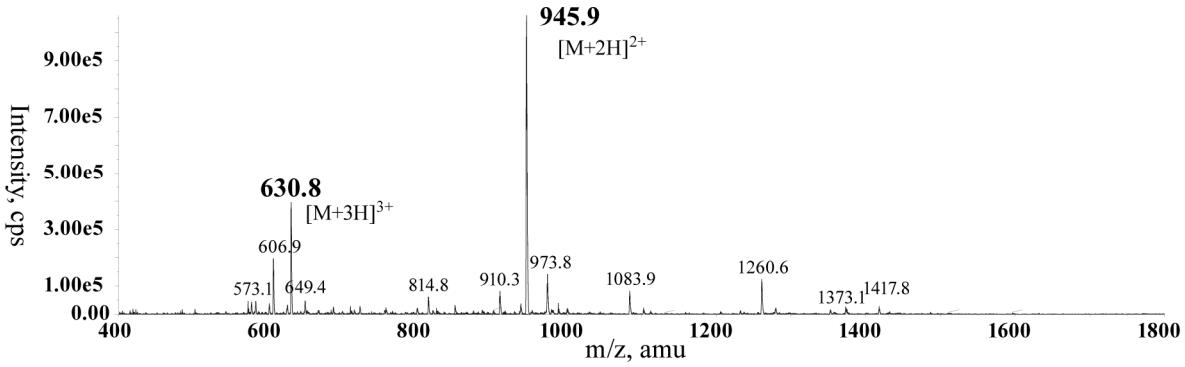

Figure 9. ES-MS of cleaved PeIA/Vc1.1. The calculated Mw for PeIA/Vc1.1 is 1889.9 g/mol, $[M+2H]^{2+}$ and $[M+3H]^{3+}$ are shown in the spectrum.

Reverse phase high performance liquid chromatography (RP-HPLC) was used to purify the peptides. PeIA/RgIA eluted after approximately 25 min and the other three peptides eluted after approximately 30 min with a 1% gradient at a flow rate of 8 ml/min. Mass spectrometry was performed on the collected HPLC samples to confirm purity and mass (Figure 10, A1, A2, A3)

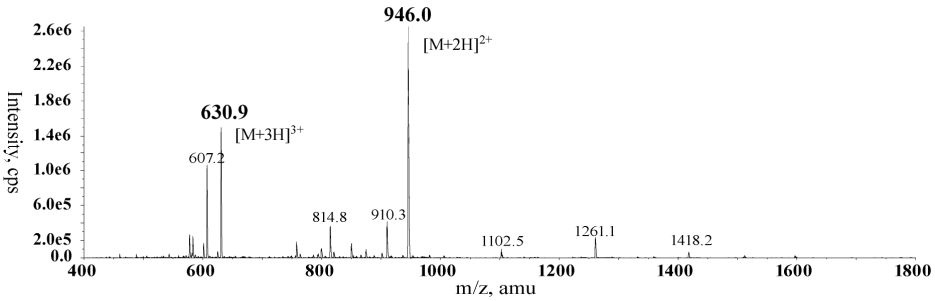

Figure 10. ES-MS of purified reduced PeIA/Vc1.1. Two major peaks corresponds to the $[M+2H]^{2+}$ and $[M+3H]^{3+}$ of PeIA/Vc1.1, which has a calculated mass of 1889.9 g/mol.

2.2 Peptide folding

The peptides were oxidized in 0.1 M NH_4HCO_3 to form the first cystine bridge between Cys^{II} and Cys^{IV}. PeIA/Vc1.1 formed polymers under the conditions used for the other three peptides (Figure 11A). To minimize the formation of polymers lower concentrations of PeIA/Vc1.1 in NH_4HCO_3 with a longer oxidation time resulted in an improved yield (Figure 11B). MALDI-MS was used to confirm the identity of the monomer. RP-HPLC and ES-MS were used to purify and identify all the partly oxidized peptides (Figure 11B, A1, A2 and A3).

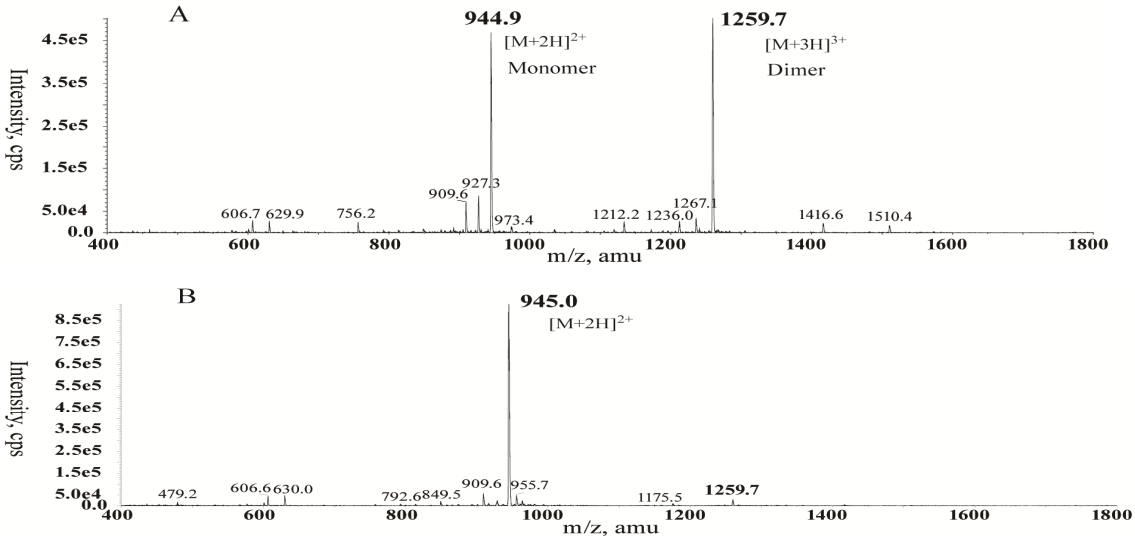

Figur 11. ES-MS spectra of PeIA/Vc1.1 oxidized in 0.1 M NH_4HCO_3. A) PeIA/Vc1.1 oxidized at a 0.1 mg/ml concentration in NH_4HCO_3 gives two major products as a result of polymer formation which was confirmed with MALDI-MS. The peak at 944.9 is the $[M+2H]^{2+}$ signal of the monomer, and the peak at 1259.5 is the $[M+3H]^{3+}$ of the dimer. B) PeIA/Vc1.1 oxidized at 0.05 mg/ml in NH_4HCO_3 gave one major product, the monomer and only a small amount of the dimer. Calculated molecular weight of partly oxidized PeIA/Vc1.1 is 1887.9 g/mol and 3775.8 g/mol for PeIA/Vc1.1 dimer.

The second cystine bridge between Cys^{I} and Cys^{III} was formed by removing the Acm groups with iodine-solution in a water bath at 37°C. The fully oxidized peptides were purified on RP-HPLC and the molecular mass was identified on ES-MS (Figure 12, A1, A2 and A3). Analytical HPLC was performed on all fully oxidized peptides to confirm purity (Figure 13, A1, A2 and A3).

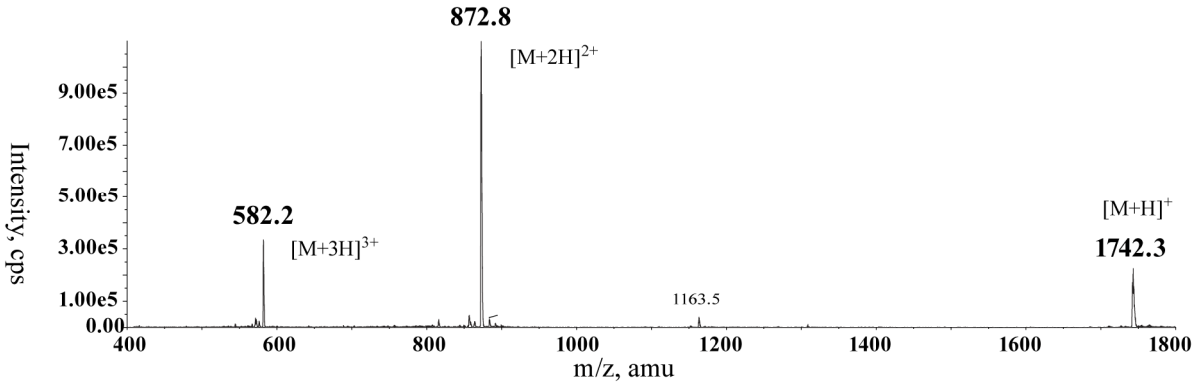

Figure 12. ES-MS of fully oxidized PeIA/Vc1.1. Calculated mass is 1745.9 g/mol, the spectre shows 3 major peaks, $[M+H]^{+}$, $[M+2H]^{2+}$ and $[M+3H]^{3+}$ of fully oxidized PeIA/Vc1.1.

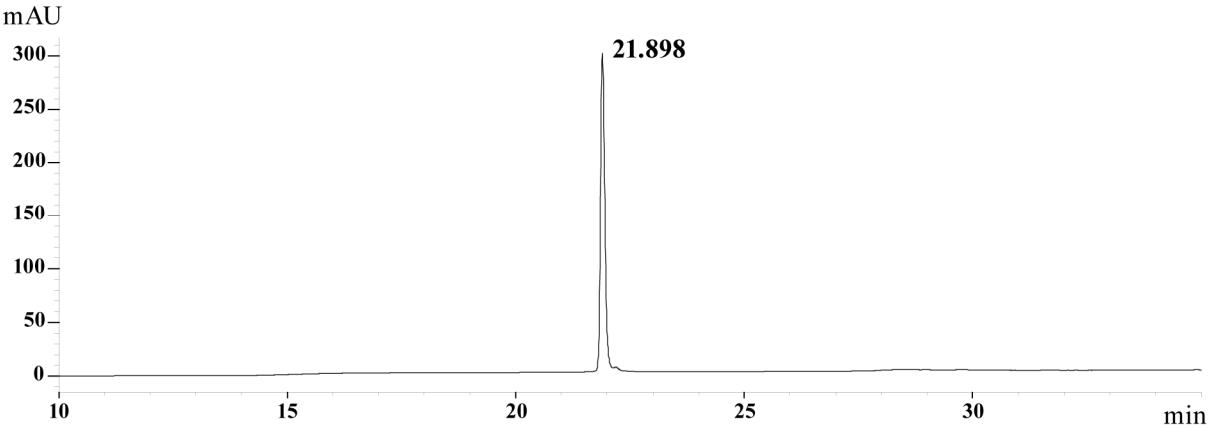

Figure 13. RP-HPLC trace of purified fully oxidized PeIA/Vc1.1 with an approximate retention time of 22 minutes.

2.3 NMR

2.3.1 Assignment of Spectra

NMR spectroscopy was used to confirm that the synthesized chimeric peptides all possessed a native fold. The proton chemical shifts were assigned by using standard methods [54].

The sequential assignment of each amino acids individual spin system was determined from Total Correlation Spectroscopy (TOCSY) spectrum by using the NH_i-NH_{i+1}, $H\alpha_i$-NH_{i+1} and

Hβ-NH_i connectivities observed in the Nuclear Overhauser Enhancement Spectroscopy (NOESY) spectrum. The sequential $H\alpha_i$-NH_{i+1} connectivities in all four peptides were obtained for the entire peptide chain except for proline residues because they lack amide protons and Gly^1-Cys^2 in PeIA/RgIA. Cys^8 in PeIA/Vc1.1 could not be assigned because of broadening of resonances in spectrum.

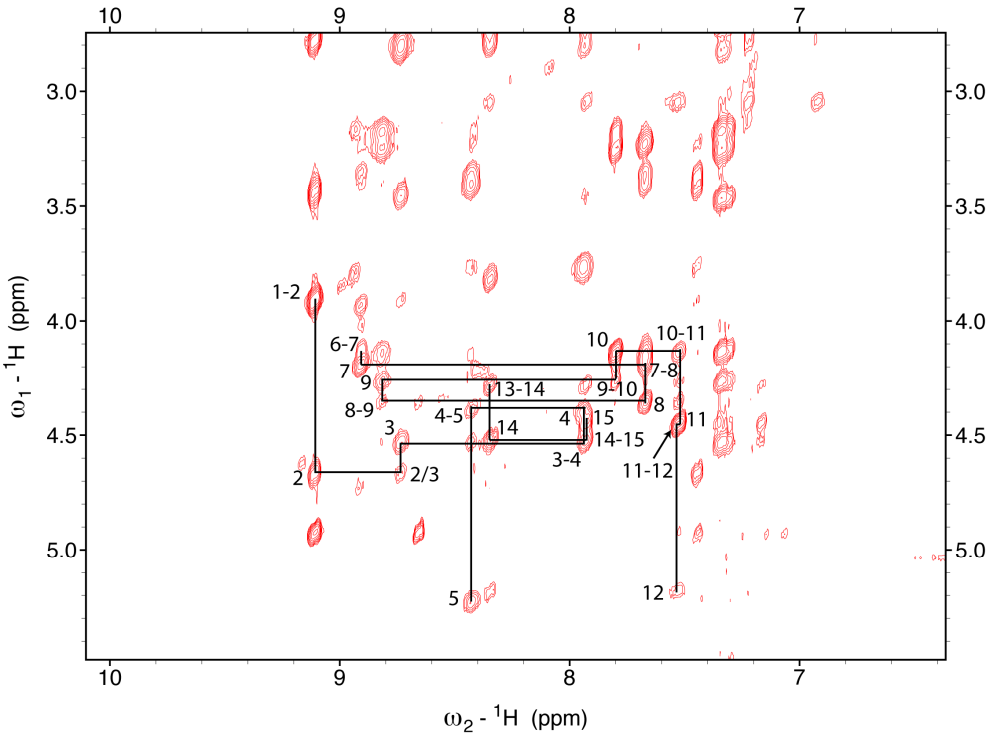

Figure 14. NOE spectrum of PeIA/AuIB showing the assignment trace of $H\alpha_i$-NH_{i+1} of all the residues except from His^5 to Pro^6 and from Asn^{12} to Pro^{13} as the Prolin lack amide protons and thereby is not detectable with NMR spectroscopy.

Secondary Hα chemical shift represents the difference between the observed Hα chemical shift and that for the corresponding residue in a random coil peptide [55]. The data obtained can supply information about the nature of the secondary structure present in the peptide. Comparison of secondary shift values between peptides provides a strong indication of similarity between the structures of the peptides. Figure 15-18 shows a comparison between secondary Hα shift for the synthesized chimeric peptides and their corresponding native peptides. Analysis of the chemical shift data show that for most of the peptides the regions from Cys^2 to Ser^4 and Pro^6 to X^{10} (X = Tyr in PeIA/Vc1.1 and PeIA/RgIA, Ala in PeIA/AuIB and Val in AuIB/PeIA) is negative, which indicates two α-helical regions around Cys^{III}.

Looking at the trends in shifts for the chimeric peptides against the native α-conotoxins illustrates a high degree of structural similarity.

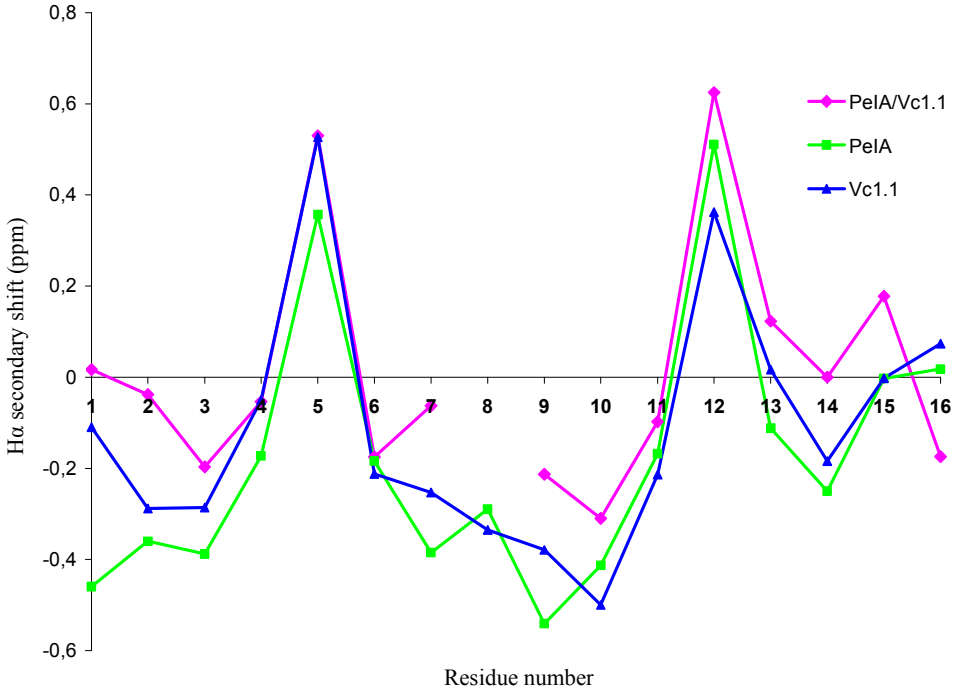

Figure 15. Secondary shift of PeIA/Vc1.1 compared to native PeIA and Vc1.1 indicating that the three dimensional structures are very similar. Cys[8] could not be assigned because of broadening of the resonances in spectrum.

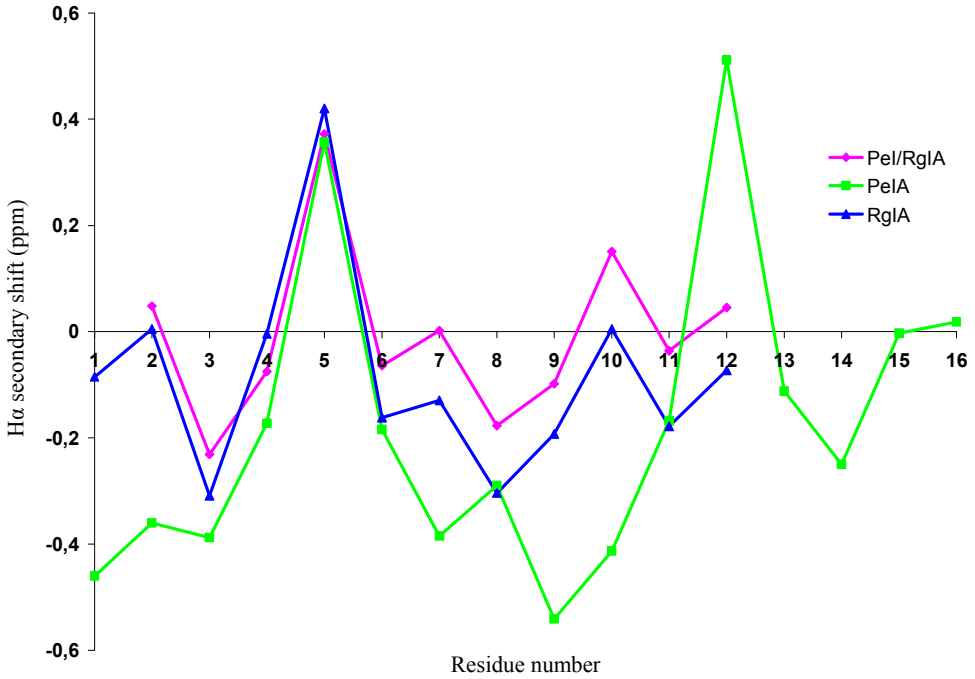

Figure 16. Secondary shift of PeIA/RgIA compared to native PeIA and RgIA indicating that the overall three dimensional structure of PeIA/RgIA is very similar to native RgIA.

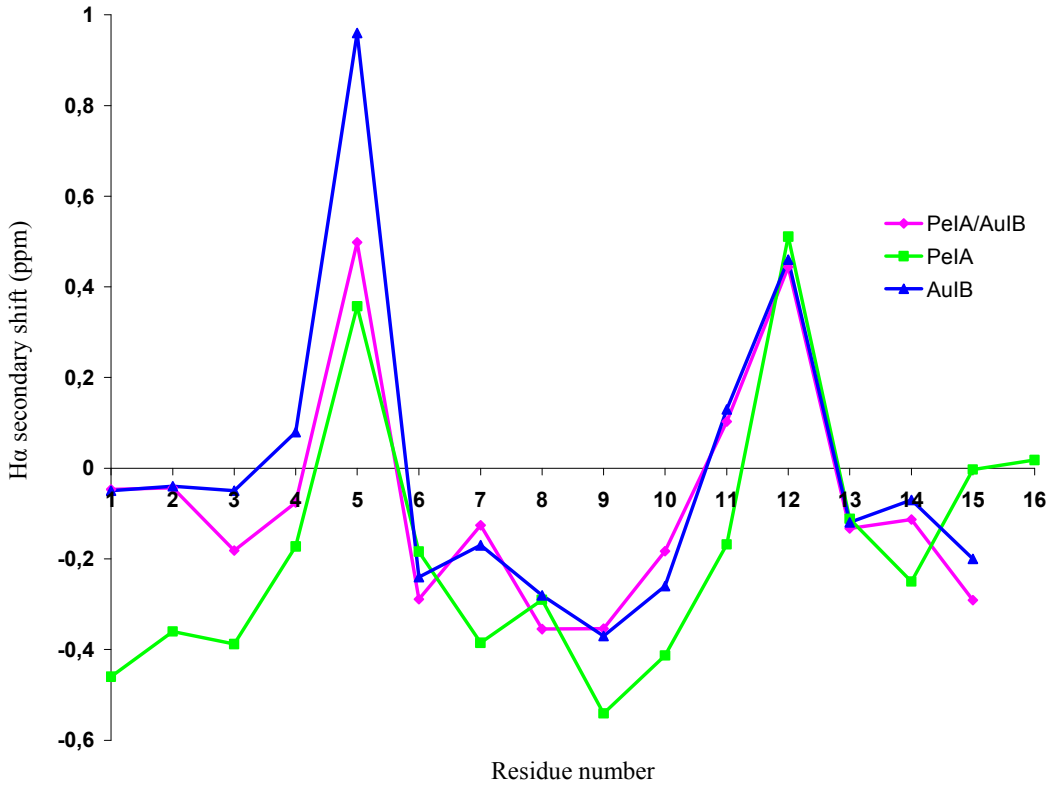

Figure 17. Secondary shift of PeIA/AuIB compared to native PeIA and AuIB indicating that the three dimensional structure of PeIA/AuIB is very similar to native AuIB and PeIA.

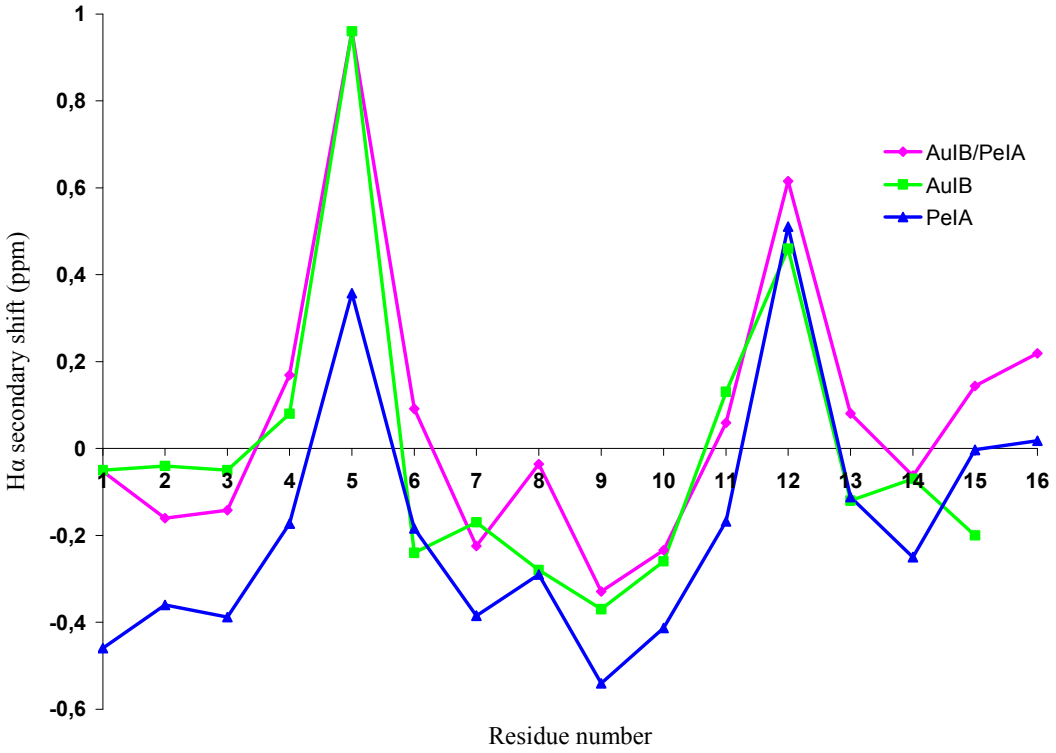

Figure 18. Secondary shift of AuIB/PeIA compared to native AuIB and PeIA indicating that the three dimensional structure of AuIB/PeIA is very similar to AuIB from residue 1-6 and to PeIA from residue 7-16.

2.3.2 Structural assignment

The three dimensional structure of PeIA/AuIB was determined by simulated annealing based on distance restraints from NOESY cross-peaks and dihedral angle restraints derived from coupling constants. The NOE-based restraints were categorized into sequential, medium and long according to distance between residues.

The restraints consist of 15 dihedral angle restraints and 93 distance restraints which include 43 sequential, 35 medium and 15 long range NOEs. 50 structures were calculated and the 20 lowest energy structures that were consistent with the experimental data were chosen for the solution structure of PeIA/AuIB. Energies and structural statistics for the 20 lowest structures are shown in table 5. All the structures were created with MOLMOL.

A total of 13 dihedral angle restraints were calculated to give the three dimensional structure, see table 4. Φ angles were determined by measuring the coupling constant $^{3}J_{H\alpha,HN}$, and the angles were restrained to -60°±30 for $^{3}J_{H\alpha\text{-}HN} < 6$ Hz and -120°±30 for $^{3}J_{H\alpha\text{-}HN} > 8$ Hz. Φ angle of six residues were included, the other angles were either overlapped or average and thereby could not be restrained. χ^{1} angles for PeIA/AuIB were determined by analyzing intraresidue NOE and $^{3}J_{H\alpha H\beta}$ coupling patterns derived from exclusive correlation spectrometry (ECOSY), seven angle restraints were included.

Table 4. Dihedral angle restraints used for the structure determination of PeIA/AuIB.

Dihedral angle restraints		Amino acid residues
□		
	- 60 ± 30	Cys^{2}, Cys^{3}, Ala^{7}, Phe^{9}, Ala^{10}
	- 120 ± 30	Cys^{8}
χ^{1}		
	- 60 ± 30	Cys^{3}, Asp^{14}, Cys^{15}
	- 180 ± 30	Cys^{2}, Cys^{8}, Phe^{9}, Asn^{12}

Table 5. Energies and structural statistics for the family of 20 lowest energy structures of PeIA/AuIB consistent with the experimental data.

Energies (kcal/mol)	
Overall	-435 ± 3
Bonds	1.36 ± 0.11
Angles	10.2 ± 1.30
Improper	2.08 ± 0.25
Van der Waals	-31.6 ± 1.38
NOE	3.54 ± 0.58
cDih	0.0915 ± 0.0221
Dihedral	76.8 ± 2.94
Electrostatic	-497 ± 5.11
RMSD	
Bond (Å)	0.0027 ± 0.00011
Angle (°)	0.44 ± 0.028
Improper (Å)	0.36 ± 0.021
NOE (Å)	0.028 ± 0.0023
cDih (Å)	0.3 ± 0.16
Atomic RMSD (Å)	
Mean global backbone	0.42 ± 0.17
Mean global heavy	0.74 ± 0.19
Distance restraints	
Intraresidue (i-j = 0)	0
Sequential (/i-j/ = 1)	43
Medium range (/i-j/ < 5)	35
Long range (/i-j/ > 5)	15
Hydrogen bonds	0
Total	93
Dihedral angle restraints	
ϕ	6
$\chi 1$	7
Total	13
Violations from experimental restraints	
NOE violations exceeding 0.2 Å	0
Dihedral violations exceeding 2.0°	0
Ramachandran Statistics	
Most favoured	87,7%
Additionally allowed	12,3%
Generously allowed	0%
Disallowed	0%

The final 20 structures are in excellent agreement with the experimental data, having no distance violations over 0.2 Å and no dihedral angle violations. Figure 19 shows the superimposed backbone structure of PeIA/AuIB with residue 2-14 in all 20 structures overlaying perfectly with a global backbone RMSD of only 0.42 ±0.17, whereas the amidated C-terminus and Gly^{1} in N-terminus is a little bit flexible. The structure confirms that the disulfide bridges are folded correctly into globular form and it shows the α-helix spanning residues Pro^{6} to Ala^{10} which is typical for native conotoxins.

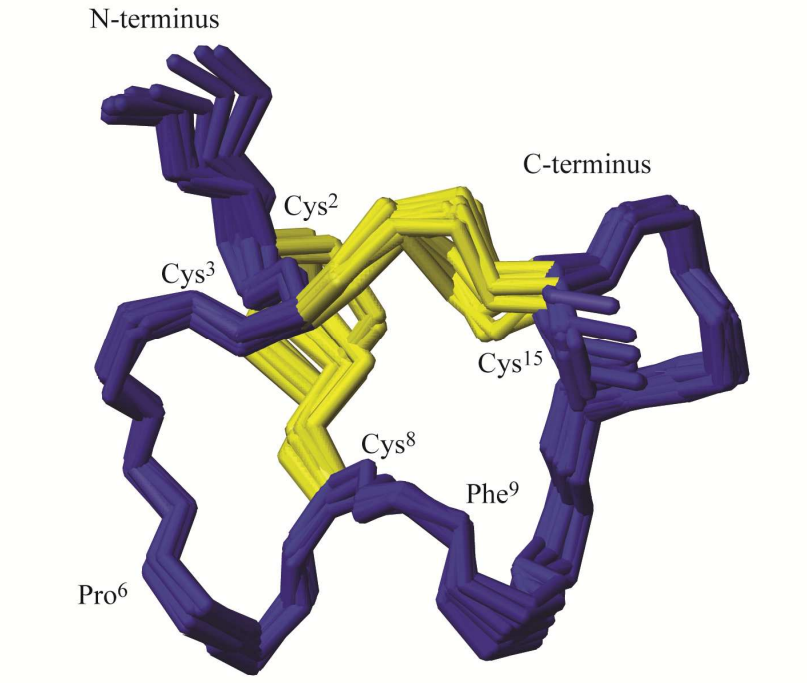

Figure 19. Three dimensional structure of PeIA/AuIB. Showing the 20 lowest energy structures in blue the superimposed backbone and the cysteine bridges in yellow. Residue 2-14 overlay perfectly, but the C-terminus is a bit flexible.

The result of these two disulfide bridges and the α-helix is a well defined structure that has the same characteristics as the native conotoxins the chimerics are derived from see Figure 20. Comparison of the three dimensional structure of PeIA/AuIB and AuIB show that they both form an α-helix around Cys^{III} and have Cys^{I} – Cys^{III} and Cys^{II} – Cys^{IV} disulfide connectivity, giving an overall fold including loop 1 and loop 2 that is very similar.

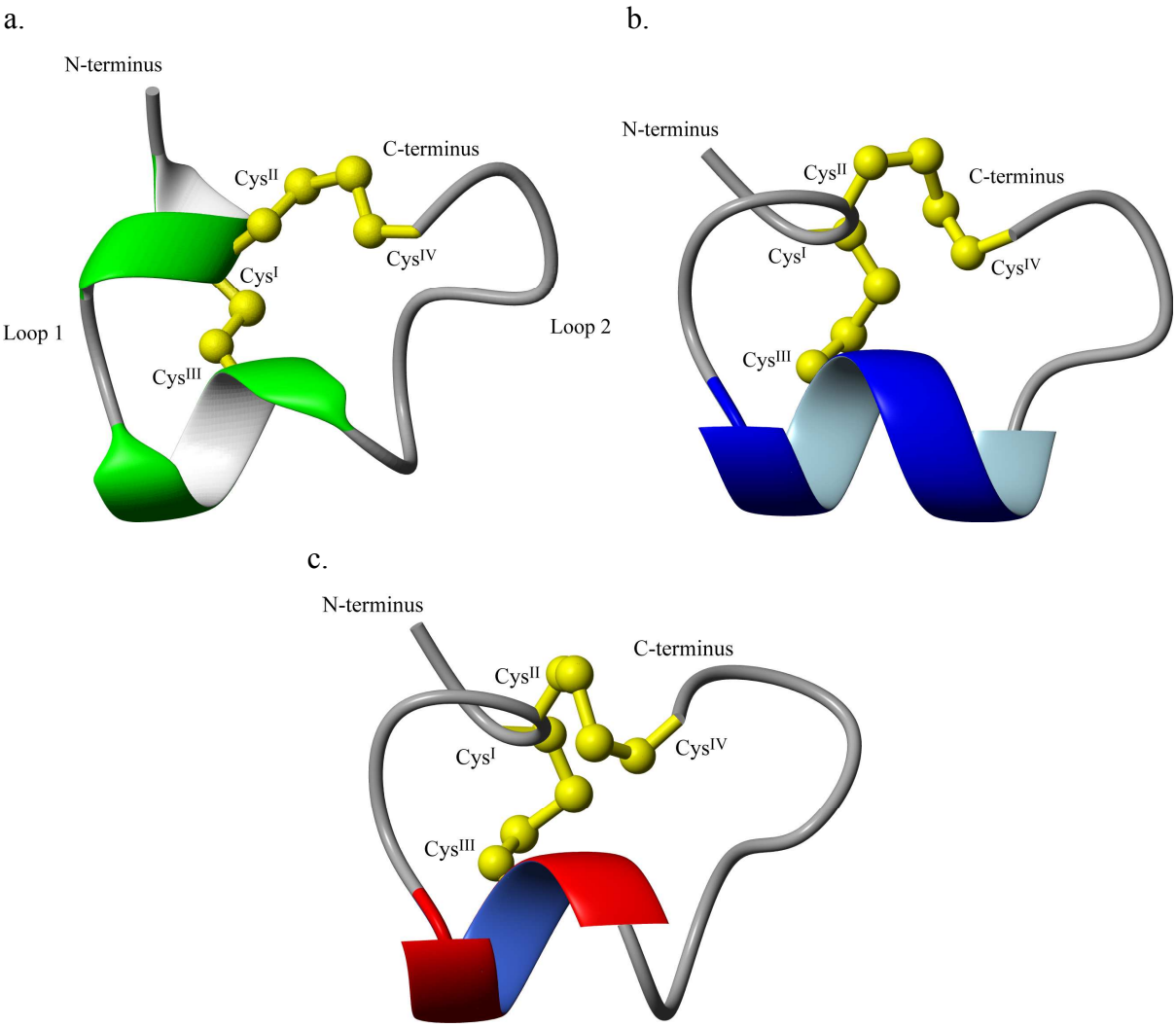

Figure 20. Comparison of three dimensional structure of chimeric PeIA/AuIB and native AuIB and PeIA showing they both have same overall fold a) Ribbon presentation of the three dimensional structure of PeIA/AuIB. The structure consists of an α-helix between Cys^2 and Ser^4 and Pro^6 and Ala^{10} between. Two cystine bridges shown as ball-sticks stabilize the structure and give the formation of loop 1 and 2. The cysteine connectivity is C^I-C^{III} and C^{II}-C^{IV}, globular. b) Ribbon presentation of the three dimensional structure of α-conotoxin AuIB. c) Ribbon presentation of the three dimensional structure of α-conotoxin PeIA.

The backbone atoms for PeIA/AuIB, PeIA and AuIB were superimposed with an RMSD between PeIA/AuIB and AuIB for the overall structure of 0,83 Å and 0,46 Å from residue 8-15 which is the region that derives from AuIB see fig. This indicates that the overall fold of the chimeric is very similar to the native conotoxins.

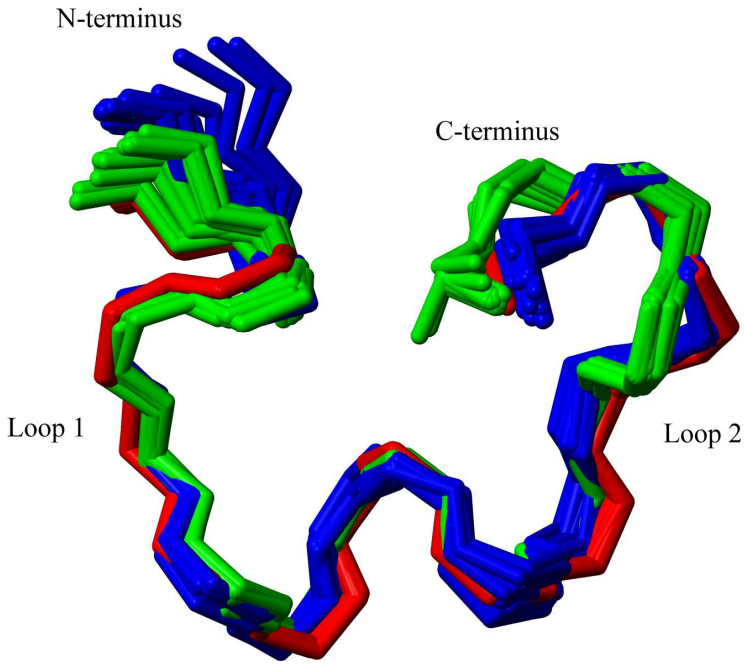

Figure 21. Superimposition of the backbone of PeIA/AuIB (blue), PeIA (green) and AuIB (red). The RMSD is 0,83 Å for residue 1-15 and 0,46 between 8-15 residue for PeIA/AuIB and AuIB indicatig that they are very similar.

2.4 Bioactivity

The concentration of peptides in solution needed to be calculated before activity assays could be prepared. The molar extinction coefficient (ε_{280}) of the peptides were calculated based on their sequence composition [56, 57]. 1740 for PeIA/Vc1.1, PeIA/RgIA, AuIB/PeIA and 250 for PeIA/AuIB (as it has no tryptophans or tyrosines). By measuring the absorbance at 280 nm the concentration of all peptides in solution was determined and 200 µg was collected and sent to our collaborator Professor David Adams at RMIT University in Melbourne for assays. The four chimeric peptides I synthesized and three chimeric peptides Chia Chia Tan prepared were tested for activity on high voltage - activated Ca^{2+} channels currents in rat dorsal root ganglion neurons against control as described previously in the literature [12]. They were tested in three different concentrations, 100 nM, 300 nM and 1 µM see Figure 16. Due to time restraints the number of replica was low (n = 3-5) but the data gives a picture of the peptide's potency. At 100 nM only PeIA/Vc1.1, Vc1.1/AuIB and AuIB/Vc1.1 show any activity. Full inhibition of the N-type Ca^{2} channels in DRG is reached for AuIB/Vc1.1, Vc1.1/PeIA, PeIA/AuIB and PeIA/Vc1.1 at 1 µM concentration.

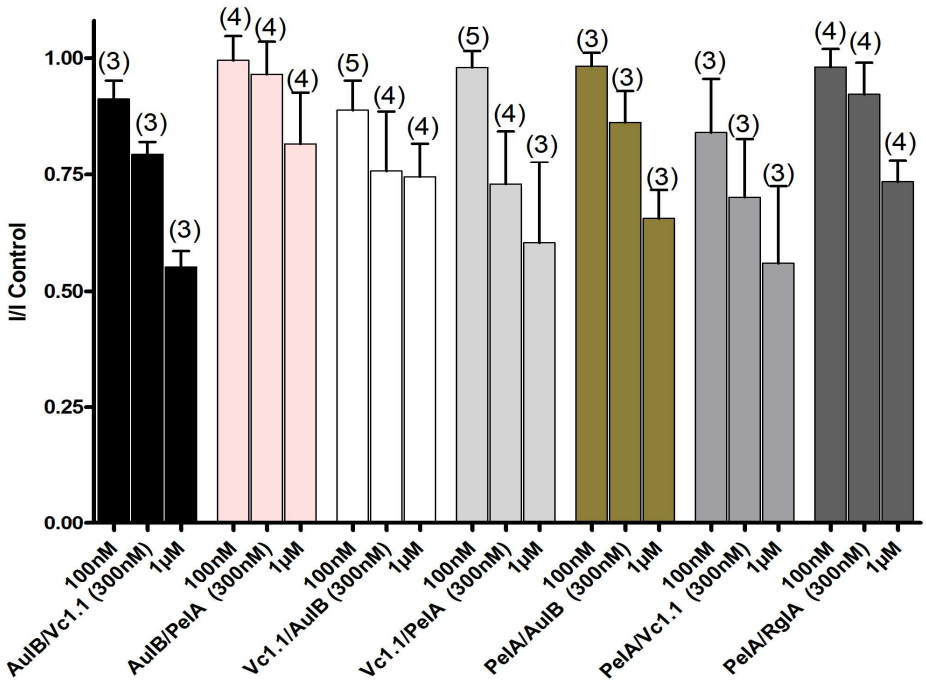

Figure 22. Bar graph of the relative inhibition of HVA Ca^{2+} channel currents by the seven chimeras at 100 nM, 300 nM and 1 µM. Numbers in parentheses reflect numbers of replica for each treatment.

Comparison of the activity to the synthesized chimeric peptides against native synthesized peptides found in the literature at 100 nM concentration show that all chimeric peptides have reduced activity Figure 17. Activity of PeIA/Vc1.1 is 83,94 ± 11,7 %, for AuIB/Vc1.1 91,49 ± 3,7 % and for Vc1.1/AuIB 88,83 ± 6,12 %.

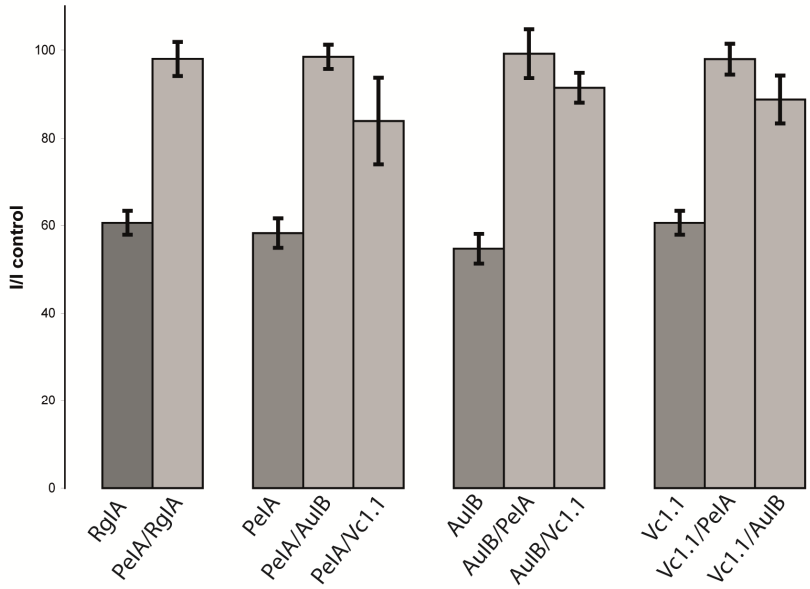

Figure 23. Relative inhibition compared to control cells of HVA Ca^{2+} currents by native α-conotoxins and chimeras at 100 nM.. All chimeras have reduced activity compared to their native α-conotoxins.

3 Discussion

Cone snails are often referred to as specialists in neuropharmacology. This is because of their sophisticated venom apparatus that consists of a mixture of venom that targets a variety of receptors in the nervous system with an exceptionally high selectivity and potency[8]. This venom consists of numerous small peptides the majority of which belong to the disulfide rich group known as conotoxins[1]. A large proportion of conotoxin's pharmacological targets are involved in pain pathways and one α-conotoxin, Vc1.1, was until recently in clinical trials for neuropathic pain. Management of neuropathic pain poses a big challenge in clinical health care settings[52]. Currently pharmacological treatment options only act on a small number of pathways and are associated with several adverse drug effects and development of tolerance[51]. α-conotoxins have excellent potential as drug leads or drugs themselves against neuropathic pain.

The small size of conotoxins makes them ideal for chemical synthesis and therefore also suitable for diverse chemical modifications, a valuable attribute for drug development. Understanding the relationship between structure and activity for a bioactive peptide is important in drug design to develop more potent and selective drugs. It reveals which residues are important for binding to the receptor and provides insight on how we can improve the potency and/or selectivity of the drug/peptide to fully exploit its potential. Thus the aim of this project was to examine the structure/activity relationship of one group of α-conotoxins that inhibits N-type Ca^{2+} channel currents via the $GABA_B$ receptor to develop more potent and selective peptides with potential as analgesic against neuropathic pain.

Changing residues in a peptide sequence can lead to drastic detrimental effects to the overall fold of the peptide. A change of just one residue can result in altered interactions between the amino acids in the sequence and result it misfolding of the peptide or alterations of the secondary and/or the three dimensional structure.
Earlier mutagenesis studies on conotoxins have observed misfolding just by changing one residue [58]. In this project we are changing both the composition and number of residues in an entire loop. Therefore the likelihood of misfolding will undoubtedly be increased. This potential hurdle was overcome to some extent by using a regioselective disulfide formation strategy. However, difficulties in folding were still evident for PeIA/Vc1.1, which formed

polymers under the first oxidation with NH_4HCO_3. Instead of the desired intramolecular disulfide bond formation between Cys^{II} and Cys^{IV} intermolecular disulfide bonds were preferred resulting in the formation of polymeric species. This can be a result of forcing the peptide to fold into conformations that may not be favourable. Making the environment less suitable for polymer formation by lowering the concentration of the peptide minimizes the probability of intermolecular disulfide bonds and this strategy was successfully employed to produce monomeric PeIA/Vc1.1.

Interestingly PeIA/Vc1.1 was the only peptide with the same amount of residues as the original peptides it was designed from. Therefore it should be able to fold the disulfide bridge with greater ease compared to PeIA/RgIA which has a size difference of four amino acids. However PeIA/RgIA displayed no signs of difficulty in folding the disulfide bridge and surprisingly did so more effectively then PelA/Vc1.1. This observation was unanticipated as we expected PeIA/RgIA to have difficulty folding the disulfide bridge.

The second aim of my project was to structurally characterize the chimeric peptides to see if they possessed a native fold. Two dimensional (2D) NMR spectroscopy experiments were performed, and the Hα chemical shifts were obtained for the entire sequence in all four peptides except Cys^{8} in PeIA/Vc1.1 and Gly^{1} in PeIA/RgIA. The spectrum of PeIA/Vc1.1 was poor and because of resonance broadening in the spectrum Cys^{8} could not be assigned. Changes in the temperature or pH-conditions can optimize the environment for different peptides and enhance the quality of the NMR spectrum. Due to time limitations this was not attempted with PeIA/Vc1.1. The trend shown by the secondary Hα shift for the other residues in PeIA/Vc1.1 compared to random coil Hα secondary shift is indicative that PeIA/Vc1.1 shares the overall fold with native conotoxins.

By looking at the trend of the secondary shifts for all the chimerics, except PeIA/RgIA, we can clearly see that they are designed by two different native peptides, with residue 1-8 coming from one conotoxin and residue 9-16 (15 for PeIA/AuIB) coming from another. For example looking at the trend in the secondary shift values for AuIB/PeIA we see that from residue Gly^{1}-Cys^{8}, corresponding to loop 1, they are similar to the secondary shift of AuIB for the same residues. At Cys^{8} the trend changes and follows the secondary shifts to PeIA from Cys^{8}-$Cys^{15/16}$ corresponding to loop 2. This indicates that they have kept the backbone

conformation of their native conotoxins and still fold correctly as native α-conotoxins with the globular connectivity and α-helix centred around Cys^8.
PeIA/RgIA has the same trend of secondary shift as RgIA throughout the sequence. This can be predicted by looking at the size of PeIA and RgIA. PeIA has 16 residues while RgIA has 12 with the change lying in loop 2. The chimeric PeIA/RgIA has 12 residues like RgIA and is therefore more likely to have a structural fold similar to RgIA.

PeIA/AuIB was picked for further structural analysis to perform a more detailed investigation of its three dimesional structure. PeIA/AuIB was shown to have the classical three dimensional fold of α-conotoxin with a helical region from residue six to ten. This confirmed the secondary shift analysis and illustrates that the chimerical conotoxins are able to form the correct α-conotoxin fold. Structure determination has to be performed on the other chimerics to confirm that they all have the characteristic α-conotoxin topology. However, the information given by the secondary shifts of the chimeras and the structural identity of PeIA/AuIB suggests that they all have a similar overall fold to the native α-conotoxins. Therefor, the structural similarity of the chimeras to the native peptides suggests that any changes in activity observed are most likely due to side-chain modifications rather than a change in the overall fold of the chimeric peptides.

The bioactivity assays shown in figure 23 illustrate that the activity is reduced for all the chimeric peptides compared to the native. Three of the chimeras have some activity at 100 nM, interestingly two of these contain Vc1.1 in loop 2 and these two peptides also show full inhibition at 1 μM. It is tempting to think that maybe Vc1.1 is more resistant to changes compared to the other native conotoxins.

Vc1.1 is a selective antagonist of the α9α10 nAChR subtype and this was thought to be the mechanism for the analgesic effect shown by Vc1.1 [59]. Studies revealed that PeIA and RgIA also targeted α9α10[60, 61]. Insight into the activity of Vc1.1 and Vc1.1 analogues suggested that α9α10 nAChRs was unlikely to be the pharmacological target for pain relief [62].
The activity of the chimeras was not tested on the nAChR's. Information acquired from such assays will provide useful knowledge for further design of a selective acting drug. Increased or decreased activity will provide information about residues that can be altered to make an analogue that is selective for the $GABA_B$ receptor with no effect on the α9α10 nAChR.

Knowledge at a molecular level on how α-conotoxins inhibit N-type Ca^{2+} channel currents via $GABA_B$ receptor is not known. Whether all four α-conotoxins interact at the same site on the $GABA_B$ receptor is not fully understood. RgIA with only 12 amino acids may bind to other sites on the receptor then the other conotoxins that contain 15-16 amino acids. In addition the similarity between loop 2 in PeIA and Vc1.1 implies that they might bind to the same site on the receptor. Ligand displacement assays and receptor mutation studies could be a potential approach to further elucidate information about the binding site of the α-conotoxins in future projects.

Proline in position 6 has been shown to be important for the analgesic activity of Vc1.1, study by Nevin et Al. shows that the [P6O] Vc1.1 analogue consisting of a modified Pro^6 to hydroxyproline has no analgesic effect [62]. This implies that proline in residue 6 is important for the analgesic effect of Vc1.1 through activation on the $GABA_B$ receptor. The importance of Pro^6 for the activity of the other α-conotoxins is currently not known, but it would be interesting to investigate as Pro^6 has also been implicated to be important for the binding of α-conotoxins to nAChR and is highly conserved in all α-conotoxins. Pro^6 inteacts with the β subunit of the nAChR through a hydrophobic interaction [63]. With PeIA, Vc1.1 and AuIB acting on α3β2 [61, 64, 65] changing Pro^6 residue could enhance selectivity for the $GABA_B$ receptor. Clearly, proline is important for the interaction between the α-conotoxins and both nAChR and $GABA_B$ receptor. Therefore understanding the structure/activity relationship at this position might provide information that can be used to design a selective analogue for each receptor.

Loop 1 differs by only 2 residues in both the native and the chimeric conotoxins. The difference in the sequence between PeIA/AuIB, Vc1.1/AuIB and AuIB (and between the other chimeric with the same loop 2 as their corresponding native peptides) is only two residues, namely position five and seven. The reduced activity shown by the bioactivity assays (Figure 23) indicate that the residues in loop 2 for each conotoxin are dependant on the residues at position five and seven to retain the activity (potency) on Ca^{2+}-channels via $GABA_B$ which further suggests that there is an interplay in between the two loops.

To further investigate if there is an interplay between the loops an alanine mutagenesis study can be performed. This can be accomplished by changing the residues at positions five and

seven one at a time in both the native and the chimeric conotoxin to an alanine and then carry out activity assays. A greater loss of activity in the native conotoxin compared to the chimeric will further support that there is interplay. The alanine analogue will disrupt the interplay in the native conotoxin while the chimeric will retain the same effect due to lack of co-operativety.

Recently two novel α-conotoxins expressed in embryos of *Conus victoriae* were characterized, Vc1.2 and Vc1.3 [66]. They also have 4 residues in loop 1, Ser^4 and Pro^6, cysteine framework I and are the same size as Vc1.1 indicating that they are likely to have the same overall fold as α-conotoxins. Interestingly one of them, Vc1.2 showed activity at $GABA_B$ receptor while Vc1.3 showed no activity. Fifteen other α-conotoxins with the same conserved primary sequence show no activity at the $GABA_B$ receptor [67]. This support the suggestion that the interaction between α-conotoxins and $GABA_B$ receptor is most likely dependent on the characteristics to the side-chains rather then the overall fold of the conotoxins.

4 Conclusion

In this study the structure/activity relationship of the α-conotoxins inhibiting high voltage activated N-type Ca^{2+} channel currents via activation of the $GABA_B$ receptor was examined by swapping the two loops between the α-conotoxins Vc1.1, PeIA, RgIA and AuIB.
The four chimeric conotoxins were successfully synthesised and folded. NMR spectroscopy was used to determine the secondary structure of the chimerics to investigate if they hold the same characteristic overall fold as the native α-conotoxins.

All four chimerics have the classical features of an α-conotoxin, with a helical region spanning from residue Pro^6 to X^{10} ((X = Tyr in PeIA/Vc1.1 and PeIA/RgIA, Ala in PeIA/AuIB and Val in AuIB/PeIA). Further structural analysis of PeIA/AuIB showed that the three dimensional structure of the chimeric conotoxin was very similar(perfect?) compared to it's native α-conotoxin. However, despite the structural similarity between the chimeric and native conotoxins, all the chimeric analogues showed reduced ability to HVA N-type Ca^{2+} currents.

The results of the structural assignment and bioactivity assays indicate that the loops cannot be swapped between α-conotoxins without a loss in activity. This loss of activity by the chimeric conotoxins indicates that there is a co-operativity between the two loops in the peptide. This study was an initial approach to gain a broad understanding of the structure/activity relationship between α-conotoxins and the $GABA_B$ receptor to facilitate the development of a selective and potent drug against neuropathic pain.

5 Material and methods

5.1 Peptide synthesis

Eight chimeric conotoxins were designed by Dr. Richard Clark, three (Vc1.1/PeIA, Vc1.1/AuIB, AuIB/Vc1.1 and AuIB/RgIA) were synthesised by Ms. Chia Chia Tan while the other four (PeIA/Vc1.1, PeIA/RgIA, PeIA/AuIB and AuIB/PeIA) were synthesized by me.

The peptides were synthesised by manual solid phase peptide synthesis (SPPS) using standard F-moc [N-(9-fluorenyl) methoxycarbonyl] chemistry. The mature native peptides have an amidated C-terminus so the resin of choice used is 4-methylbenzhydrylamine (MBHA) - rink amide resin. Acetamidomethyl (Acm) protection groups were incorporated on two Cysteines (C2 and C4) to facilitate regioselective disulfide formation, the other two cysteines had (-trt) protection group. The side-chain protection of non-cysteine residues was Fmoc-Arg(pbf)-OH, Fmoc-Asn(trt)-OH, Fmoc-Asp(OtBu)-OH, Fmoc-Glu(OtBu)-OH, Fmoc-His(trt)-OH, Fmoc-Ser(tBu)-OH, Fmoc-Thr(tBu)-OH, Fmoc-Tyr(tBu)-OH

All the peptides was synthesised on a 0.25 mmole scale. The amount of resin needed was calculated by using the substitution value for the resin (number of mmoles per gram of resin) and the scale in mmole; mass of resin required = scale in mmole/substitution value.
The resin was prepared by soaking it in dimethylformamide (DMF) for 1-2 hours before it was placed in the reaction vessel. Then it was washed with DMF and treated with piperidine (2 x 1 min) to remove the Fmoc protection groups, followed by thoroughly washing with DMF to remove all traces of piperidine. The amino acids are activated by adding a solution of 0.5 M HBTU and diisopropylethylamine (DIPEA) in DMF in amounts according to the scale the peptide is synthesised (2 ml 0.5 M HBTU in DMF and 174 µl DIPEA when 0.25 mmole scale). The activated amino acid was added the deprotected resin and allowed to react for a minimum of 10 min.
The yield percentage of every amino acid coupling should be > 99.6 % (or 99 % for a short peptide), and this was checked by a ninhydrin test [68]. To perform the test (3-5 mg) resin was weighed into a test tube and 2 drops of 76% w/w phenol in ethanol, 4 drops of 0.2 mM KCN in pyridine and 2 drops of 0.28 M ninhydrin in ethanol was added. A control tube containing no resin was also prepared. The samples were incubated for 5 min at 100°C and then added 2.8 ml of 60% ethanol in water. When the resin was settled the absorbance of the

solution with resin against the control was measured at 570 nm. To calculate the coupling following formula was used:

% coupling yield = 100 x (1-(A_{570} x 200/SV x mass of resin))

The coupling yield to proline cannot be detected by the ninhydrin test, because the test detects the primary amine remaining and the N-termini of proline is a secondary amine. The amino acids after a proline residue was double coupled. If the yield was still poor after recoupling an acetylation was preformed to cap any unreacted amine groups. For acetylation the resin was treated with a mixture of 870 µL acetic anhydride, 470 µL DIPEA and 15 ml DMF for 2 x 5 min.

The peptides were cleaved from the solid phase resin using a mixture of trifluoracetic acid (TFA), TIPS (tri-isopropylsilane), DODT (3, 6 – dioxa – 1, 8 – octanedithiol) and H_2O (90/5/2.5/2.5 v/v) at room temperature for two hours. TFA cleaves the peptide from the resin while DODT and TIPS work as scavengers. TFA was evaporated under vacuum. Cold diethyl ether was then added to precipitate the peptide and Buffer A/B (Buffer A; H_2O/ 0,05% TFA, Buffer B; 90% CH_3CN/ 10% H_2O/ 0,045% TFA) was added to separate the peptide from the scavengers. Residual ether was removed from the aqueous layer by rotary evaporation. A MS of the resulting solution was run to determine the purity and molecular weight of the cleaved peptides and the mixture was then lyophilised.

The crude peptide was purified by RP-HPLC (reverse phase high performance liquid chromatography) with a C_{18} column at a flow rate of 8 ml/min using a 1 % gradient, (0-80% Buffer B in 80 min, Buffer A = 0.05% TFA in H_2O, Buffer B = 90% acetonitrile in H_2O (v/v) with 0.045% TFA). ES-MS was used to identify the peptides in the HPLC fractions and the fractions containing the desired product were combined and lyophilised, before the resulting reduced peptide was weighed.

5.2 Peptide folding

The reduced peptides were oxidized in 0.1 M NH_4HCO_3 (pH 8, at 0.1 mg/ml peptide concentration), to form the disulfide bridge between C^I and C^{III}. The reaction was stirred overnight at room temperature. For PeIA/Vc1.1 the concentration was 0.05 mg/ml and it

stood on stirrer for three days. Purification was achieved by RP-HPLC followed by identification by ES-MS and Maldi-MS.

The second disulfide bond was formed by oxidation in iodine solution at low pH to form the second disulfide bridge between the Acm-protected cysteines C^{II} and C^{IV}. The peptides were dissolved in Buffer A at 1 mg/ml concentration and incubated in a water bath at 37° C. Iodine in acetonitrile was dripped in until the solution was orange/yellow. The solution was allowed to react for 5 min and then stopped by addition of ascorbic acid until the solution turned colourless. The fully oxidized peptide was filtered and HPLC was performed for purification. HPLC samples were identified by ES-MS and run on analytical HPLC to confirm purity.

5.3 NMR spectroscopy

5.3.1 Spectral assignment

NMR data was used to analyze the backbone/secondary structure of all the chimeras. The peptides were dissolved in 90 % H_2O (500 µL Milli – Q water) and 10 % D_2O (50 µL). ^1H, TOCSY and NOESY spectra were acquired at 280 K on a BRUKER 600- MHz spectrometer for PeIA/RgIA, PeIA/AuIB and PeIA/Vc1.1 while ^1H, TOCSY and NOESY spectra were acquired at 310 K on a BRUKER 500- MHz spectrometer for AuIB/PeIA. TOCSY and NOESY spectra were recorded with 200 ms mixing time. All the spectra were analyzed with Sparky software and assigned using the sequential assignment technique.

5.3.2 Structural assignment

COSY and NOESY (200 or 100 ms mixing time) spectra were obtained on a BRUKER 600-MHz spectrometer at 280 K. The peptide was dissolved in 90 % H_2O (500 µL Milli – Q water) and 10 % D_2O (50 µL). ECOESY, TOCSY and 1D spectra were recorded on a BRUKER 500- MHz spectrometer at 280 K. The peptide was dissolved in 100 % D_2O. Information of slowly exchanging amide protons was acquired by data of 1D and TOCSY spectra immediately upon dissolution of a fully protonated peptide in D_2O. All spectra were assigned using the sequential assignment technique.

NOE peak heights in the 200ms NOESY spectra were translated into distance restraints with the appropriate pseudoatom corrections using CYANA. Backbone dihedral angle restraints were derived from $^{3}J_{H\alpha,HN}$ coupling constants measured directly from 1D spectra. Angles were restrained to -60°±30 for $^{3}J_{H\alpha\text{-}HN} < 6$ Hz and -120°±30 for $^{3}J_{H\alpha\text{-}HN} > 8$ Hz. Intraresidue NOE and $^{3}J_{H\alpha H\beta}$ coupling patterns derived from ECOSY was used in assigning χ^{1} angle conformation of side chains. Initial structure was calculated by using CYANA software. Afterwards CNS software was used to derive a structure in more natural environment. Fifty structures were calculated and the 20 structures with lowest energy which had no violations of NOE > 0.2 Å or dihedral angle restraints > 2.0 ° were retained for analysis. Structures were visualized with the program MOLMOL.

5.4 Determining the concentration of a peptide solution

The concentration of the peptides was determined by UV absorption and a calculated extinction coefficient of the peptide at 280 nm (ε_{280}). The absorbance of peptides is determined by number of tryptophans (n_{Trp}), tyrosines (n_{Tyr}) and disulfide bonds ($n_{s\text{-}s}$) in the sequence. The ε for a peptide in solution can be calculated by this formula;

$$\varepsilon_{280} = (5500 \times n_{Trp}) + (1490 \times n_{Tyr}) + (125 \times n_{s\text{-}s})$$

The absorbance was measured at 280 nm and the concentration was calculated by using Beer-Lambert Law ($A = \varepsilon \times C \times l$) where A is the absorbance, ε is the molar extinction coefficient ($M^{-1}cm^{-1}$), C is the peptide concentration (M) and l is the pathlenght (cm).

5.5 Bioactivity

Bioactivity of PeIA/Vc1.1, PeIA/RgIA, PeIA/AuIB and AuIB/PeIA were assessed by measuring electrophysiological currents from voltage gated Ca^{2+} channels in Dorsal root ganglion neurons from rat. The assays were done in the laboratory of our collaborator Professor David Adams at RMIT University in Melbourne.

5.6 Analytical instruments

5.6.1 Preparative and Semipreparative HPLC

All preparative and semipreparative HPLC were performed on one of these following machines:

- Waters 600-MS System Controller equipped with a Waters 484 Tunable Absorbance Detector and Delta 5.5 chromatography data system software
- Waters 600 Controller equipped with a Waters 600 pump and a Waters 2487 Dual λ Absorbance Detector and Empower software
- Waters 600E System Controller equipped with a Waters 484 Tunable Absorbance Detector Empower software
- Shimadzu LC-20AT prominence liquid chromatography equipped with a SPD-20A prominence UV/VIS detector and LC solutions software
- Shimadzu LC-20AT prominence liquid chromatography equipped with a SPD-M20A diode array detector and LC solutions software

All preparative HPLC samples were manually loaded onto Phenomenex Jupiter C_{18} (250 x 21.20 mm, 300 Å pore size, 15 μm particle size) or VYDAC Protein & Peptide C_{18} (250 x 22 mm, 300 Å pore size, 10 μm particle size) with UV detection at 215 nm. Reduced peptide samples were eluted at a flow rate of 8 ml/min with a linear gradient of 0-80 % Buffer B for 80 min while partly oxidised and fully oxidised peptide samples were eluted at a flow rate of 8 ml/min with a linear gradient of 0-80 % Buffer B for 160 min.

For semipreparative HPLC the samples were manually loaded onto 3 ml/min Phenomenex Jupiter C18 (250 x 10.00 mm 5 micron, 300 Å pore size, 5 μm particle size) with UV detector at 215 nm. Samples were eluted at a flow rate of 3 ml/min with a linear gradient of 0-80 % Buffer B for 320 min.

5.6.2 Analytical HPLC

All analytical HPLC were performed on an Agilent 1100 series with ChemStation software?. Samples were injected into a Phenomenex Jupiter C18 column (150 x 2.00 mm 5 micron, 300

Å pore size, 5 ìm particle size) and eluted at a flow rate of 0.3 ml/min with a linear gradient of 0-80% Buffer B for 40 min with UV detector at 215 nm.

5.6.3 Mass spectrometry

ES-MS

The identification of all HPLC constituents was based on mass and all the mass data was obtained from an ABSciex API2000 mass spectrometer with analyst software. 5-10 µL was injected.

MALDI-MS

All MALDI mass spectrometry were performed on a Voyager STR MALDI-TOF mass spectrometer with Voyager instrument Control Software.

6 Appendix

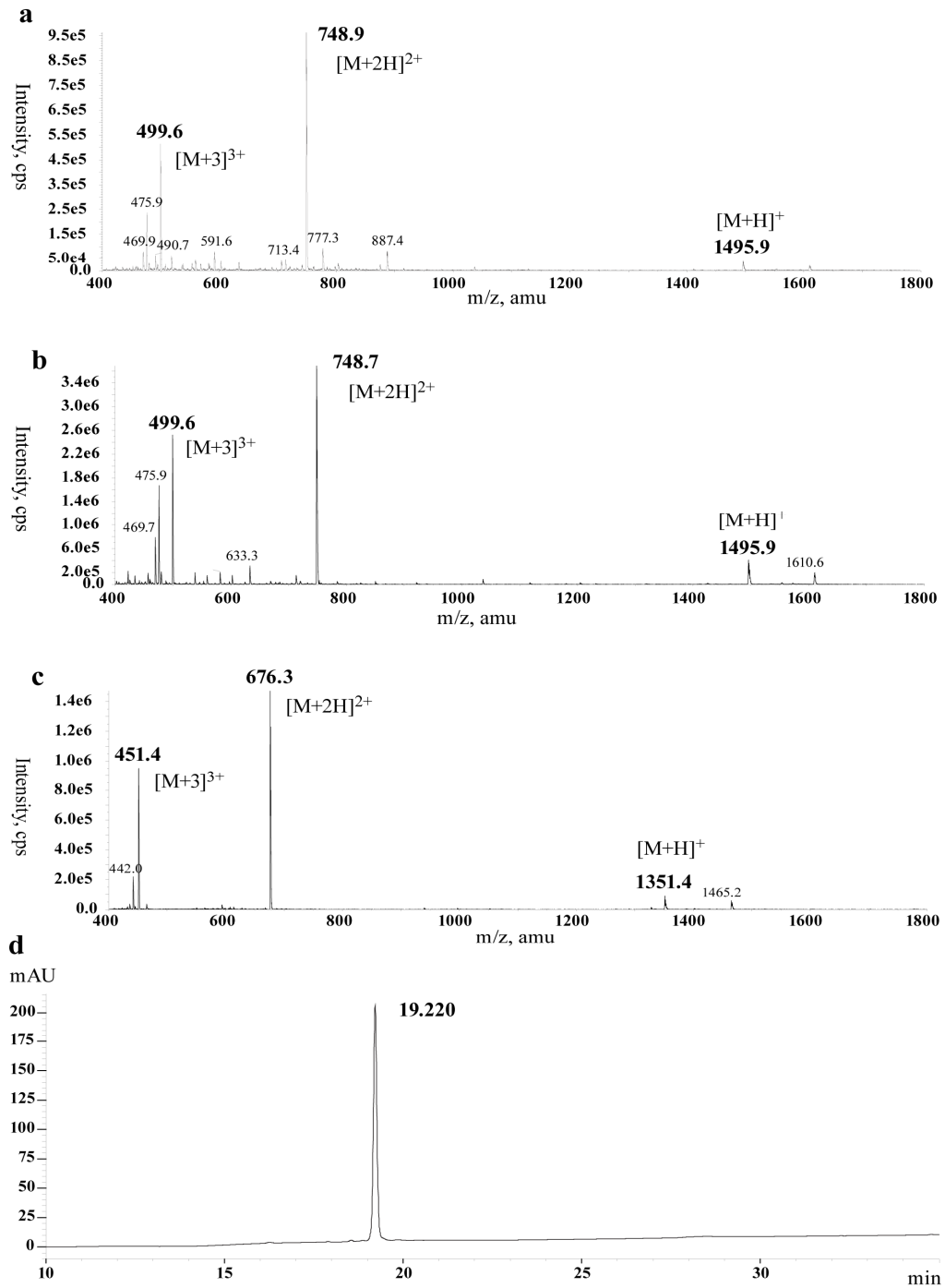

Figure A1. a) ES-MS of cleaved PeIA/RgIA showing three major peaks corresponding to $[M+H]^{+}$, $[M+2H]^{+2}$ and $[M+3H]^{+3}$ of PeIA/RgIA. Calculated mass is 1496.5 g/mol b) ES-MS of purified reduced PeIA/RgIA showing three major peaks corresponding to $[M+H]^{+}$, $[M+2H]^{+2}$ and $[M+3H]^{+3}$ of PeIA/RgIA. The calculated mass is 1496.5 g/mol. c) ES-MS of fully oxidised PeIA/RgIA showing three major peaks corresponding to $[M+H]^{+}$, $[M+2H]^{+2}$ and $[M+3H]^{+3}$ of PeIA/RgIA. Calculated mass is 1352.5 g/mol d) RP-HPLC trace of purified fully oxidised PeIA/RgIA with retention time of approximately 19 minutes.

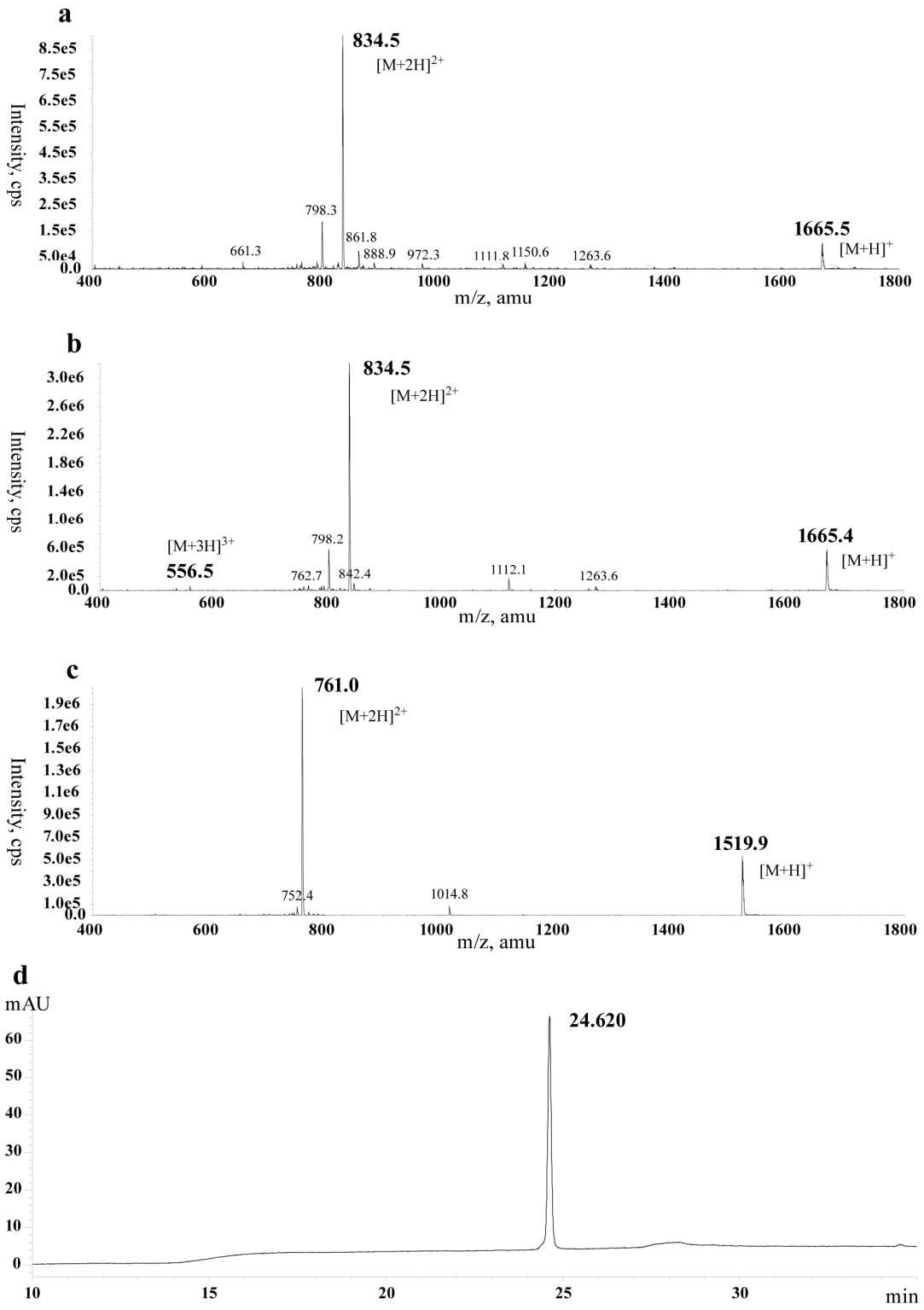

Figure A2. a) ES-MS of cleaved PeIA/AuIB showing two major peaks corresponding to the $[M+H]^{+}$ and $[M+2H]^{+2}$ of PeIA/AuIB. Calculated mass is 1666.7 g/mol b) ES-MS of purified reduced PeIA/AuIB showing three peaks corresponding to the $[M+H]^{+}$, $[M+2H]^{+2}$ and $[M+3H]^{+3}$ of PeIA/AuIB. The calculated mass is 1666.7 g/mol. c) ES-MS of fully oxidised PeIA/AuIB showing two major peaks corresponding to the $[M+H]^{+}$ and $[M+2H]^{+2}$ and of PeIA/AuIB. Calculated mass is 1522.7 g/mol d) RP-HPLC trace of purified fully oxidised PeIA/AuIB with retention time of approximately 25 minutes.

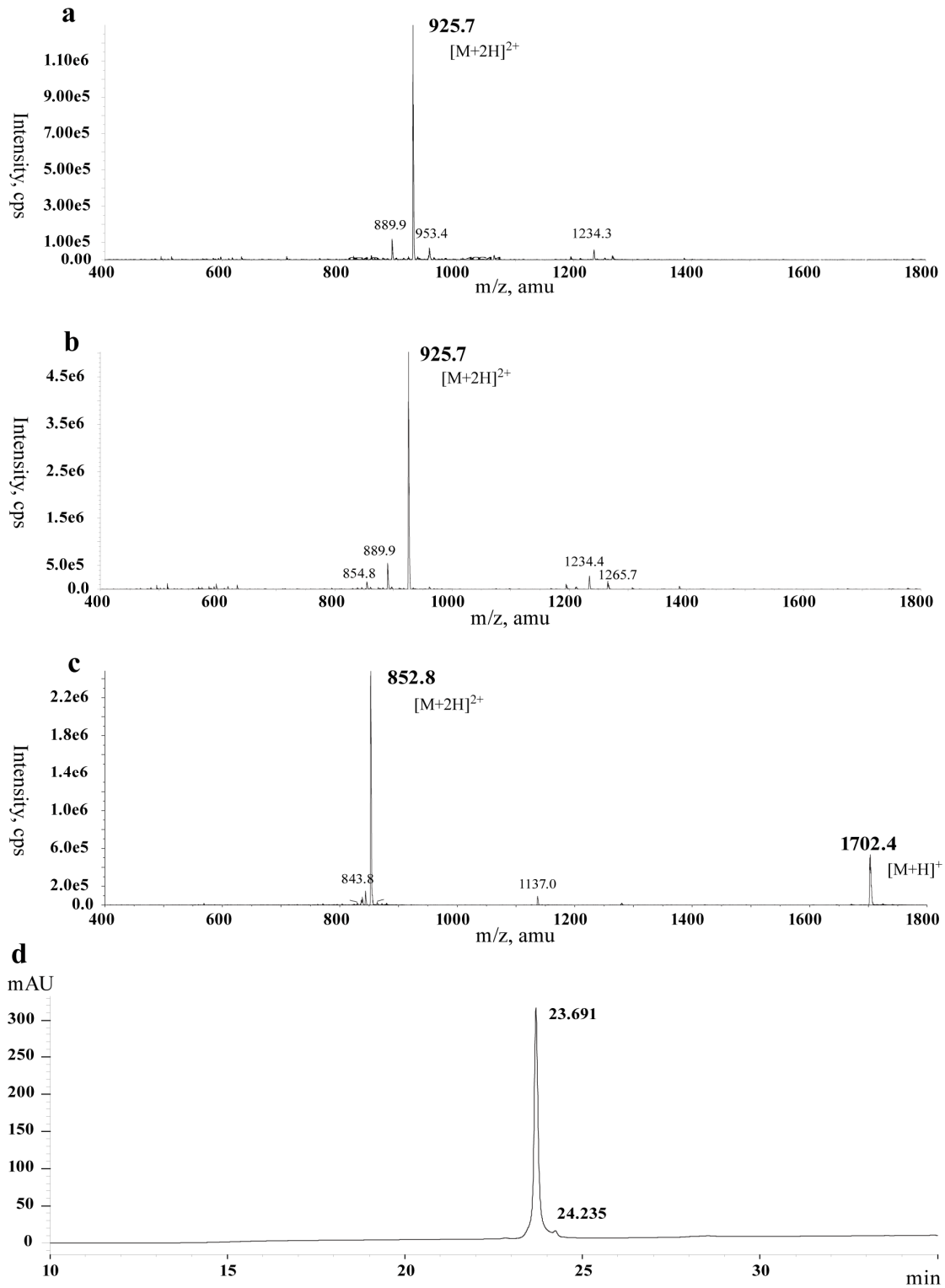

Figure A3. a) ES-MS of cleaved AuIB/PeIA showing one major peak corresponding to the $[M+2H]^{+2}$ of AuIB/PeIA. Calculated mass is 1849.9 g/mol b) ES-MS of purified reduced AuIB/PeIA showing one peak corresponding to the $[M+H]^{+}$ of AuIB/PeIA. The calculated mass is 1849.9 g/mol. c) ES-MS of fully oxidised AuIB/PeIA showing two major peaks corresponding to the $[M+H]^{+}$ and $[M+2H]^{+2}$ of AuIB/PeIA. Calculated mass is 1705.9 g/mol d) RP-HPLC trace of purified fully oxidised AuIB/PeIA with retention time of approximately 25 minutes.

7 References

1. Halai, R. and D.J. Craik, *Conotoxins: natural product drug leads.* Nat Prod Rep, 2009. **26**(4): p. 526-36.
2. Terlau, H. and B.M. Olivera, *Conus venoms: a rich source of novel ion channel-targeted peptides.* Physiol Rev, 2004. **84**(1): p. 41-68.
3. Hermitte, L.C., *Venomous marine molluscs of the genus Conus.* Trans R Soc Trop Med Hyg, 1946. **39**: p. 485-512.
4. Kohn, A.J., *Cone shell stings; recent cases of human injury due to venomous marine snails of the genus Conus.* Hawaii Med J, 1958. **17**(6): p. 528-32.
5. Kohn, A.J., P.R. Saunders, and S. Wiener, *Preliminary studies on the venom of the marine snail Conus.* Ann N Y Acad Sci, 1960. **90**: p. 706-25.
6. Olivera, B.M., et al., *Peptide neurotoxins from fish-hunting cone snails.* Science, 1985. **230**(4732): p. 1338-43.
7. Olivera, B.M., *Conus venom peptides: Reflections from the biology of clades and species.* Annual Review of Ecology and Systematics, 2002. **33**: p. 25-47.
8. Olivera, B.M. and R.W. Teichert, *Diversity of the neurotoxic Conus peptides: a model for concerted pharmacological discovery.* Mol Interv, 2007. **7**(5): p. 251-60.
9. Alonso, D., et al., *Drugs from the sea: conotoxins as drug leads for neuropathic pain and other neurological conditions.* Mini Rev Med Chem, 2003. **3**(7): p. 785-7.
10. Cruz, L.J., Gray, W. R., Yoshikami, D., Olivera, B. M, *Conus venoms: a rich source of neuroactive peptides.* J. Toxicol. - Toxin Rev, 1985. **4**: p. 107-132.
11. Olivera, B.M., *Conus peptides: biodiversity-based discovery and exogenomics.* J Biol Chem, 2006. **281**(42): p. 31173-7.
12. Callaghan, B., et al., *Analgesic alpha-conotoxins Vc1.1 and Rg1A inhibit N-type calcium channels in rat sensory neurons via GABAB receptor activation.* J Neurosci, 2008. **28**(43): p. 10943-51.
13. Schmidtko, A., et al., *Ziconotide for treatment of severe chronic pain.* Lancet, 2010. **375**(9725): p. 1569-77.
14. Cruz, L.J., W.R. Gray, and B.M. Olivera, *PURIFICATION AND PROPERTIES OF A MYOTOXIN FROM CONUS-GEOGRAPHUS VENOM.* Archives of Biochemistry and Biophysics, 1978. **190**(2): p. 539-548.
15. Dutton, J.L. and D.J. Craik, *alpha-Conotoxins: nicotinic acetylcholine receptor antagonists as pharmacological tools and potential drug leads.* Curr Med Chem, 2001. **8**(4): p. 327-44.
16. Adams, D.J., et al., *Conotoxins and their potential pharmaceutical applications.* Drug Development Research, 1999. **46**(3-4): p. 219-234.
17. Marx, U.C., N.L. Daly, and D.J. Craik, *NMR of conotoxins: structural features and an analysis of chemical shifts of post-translationally modified amino acids.* Magn Reson Chem, 2006. **44 Spec No**: p. S41-50.
18. Albuquerque, E.X., et al., *Mammalian nicotinic acetylcholine receptors: from structure to function.* Physiol Rev, 2009. **89**(1): p. 73-120.

19. Klimis, H., et al., *A novel mechanism of inhibition of high-voltage activated calcium channels by alpha-conotoxins contributes to relief of nerve injury-induced neuropathic pain.* Pain, 2011. **152**(2): p. 259-66.
20. Daly, N.L., et al., *Structure and Activity of {alpha}-Conotoxin PeIA at Nicotinic Acetylcholine Receptor Subtypes and GABAB Receptor-coupled N-type Calcium Channels.* J Biol Chem, 2011. **286**(12): p. 10233-7.
21. Bettler, B., et al., *Molecular structure and physiological functions of GABA(B) receptors.* Physiological Reviews, 2004. **84**(3): p. 835-867.
22. Ulrich, D. and B. Bettler, *GABA(B) receptors: synaptic functions and mechanisms of diversity.* Curr Opin Neurobiol, 2007. **17**(3): p. 298-303.
23. Martin, S.C., S.J. Russek, and D.H. Farb, *Molecular identification of the human GABABR2: cell surface expression and coupling to adenylyl cyclase in the absence of GABABR1.* Mol Cell Neurosci, 1999. **13**(3): p. 180-91.
24. Kuner, R., et al., *Role of heteromer formation in GABAB receptor function.* Science, 1999. **283**(5398): p. 74-7.
25. Jones, K.A., et al., *GABA(B) receptors function as a heteromeric assembly of the subunits GABA(B)R1 and GABA(B)R2.* Nature, 1998. **396**(6712): p. 674-9.
26. Kaupmann, K., et al., *GABA(B)-receptor subtypes assemble into functional heteromeric complexes.* Nature, 1998. **396**(6712): p. 683-7.
27. White, J.H., et al., *Heterodimerization is required for the formation of a functional GABA(B) receptor.* Nature, 1998. **396**(6712): p. 679-82.
28. Ng, G.Y., et al., *Identification of a GABAB receptor subunit, gb2, required for functional GABAB receptor activity.* J Biol Chem, 1999. **274**(12): p. 7607-10.
29. Brauner-Osborne, H., P. Wellendorph, and A.A. Jensen, *Structure, pharmacology and therapeutic prospects of family C G-protein coupled receptors.* Curr Drug Targets, 2007. **8**(1): p. 169-84.
30. Cousins, M.S., D.C. Roberts, and H. de Wit, *GABA(B) receptor agonists for the treatment of drug addiction: a review of recent findings.* Drug Alcohol Depend, 2002. **65**(3): p. 209-20.
31. Xi, Z.X. and E.A. Stein, *Baclofen inhibits heroin self-administration behavior and mesolimbic dopamine release.* J Pharmacol Exp Ther, 1999. **290**(3): p. 1369-74.
32. Smith, G.D., et al., *Increased sensitivity to the antinociceptive activity of (+/-)-baclofen in an animal model of chronic neuropathic, but not chronic inflammatory hyperalgesia.* Neuropharmacology, 1994. **33**(9): p. 1103-8.
33. McCarson, K.E. and S.J. Enna, *Nociceptive regulation of GABA(B) receptor gene expression in rat spinal cord.* Neuropharmacology, 1999. **38**(11): p. 1767-73.
34. Branden, L., et al., *The novel, peripherally restricted GABAB receptor agonist lesogaberan (AZD3355) inhibits acid reflux and reduces esophageal acid exposure as measured with 24-h pHmetry in dogs.* Eur J Pharmacol, 2010. **634**(1-3): p. 138-41.
35. Lehmann, A., *GABAB receptors as drug targets to treat gastroesophageal reflux disease.* Pharmacol Ther, 2009. **122**(3): p. 239-45.
36. Slattery, D.A., S. Desrayaud, and J.F. Cryan, *GABAB receptor antagonist-mediated antidepressant-like behavior is serotonin-dependent.* J Pharmacol Exp Ther, 2005. **312**(1): p. 290-6.

37. Froestl, W., et al., *SGS742: the first GABA(B) receptor antagonist in clinical trials.* Biochem Pharmacol, 2004. **68**(8): p. 1479-87.
38. Nakagawa, Y., A. Sasaki, and T. Takashima, *The GABA(B) receptor antagonist CGP36742 improves learned helplessness in rats.* Eur J Pharmacol, 1999. **381**(1): p. 1-7.
39. Bowery, N.G., et al., *Baclofen: a selective agonist for a novel type of GABA receptor]proceedings]*. Br J Pharmacol, 1979. **67**(3): p. 444P-445P.
40. Campbell, S.K., et al., *The effects of intrathecally administered baclofen on function in patients with spasticity.* Phys Ther, 1995. **75**(5): p. 352-62.
41. Treede, R.D., et al., *Neuropathic pain: redefinition and a grading system for clinical and research purposes.* Neurology, 2008. **70**(18): p. 1630-5.
42. Bouhassira, D., et al., *Prevalence of chronic pain with neuropathic characteristics in the general population.* Pain, 2008. **136**(3): p. 380-7.
43. Torrance, N., et al., *The epidemiology of chronic pain of predominantly neuropathic origin. Results from a general population survey.* J Pain, 2006. **7**(4): p. 281-9.
44. Jensen, T.S., et al., *The clinical picture of neuropathic pain.* Eur J Pharmacol, 2001. **429**(1-3): p. 1-11.
45. Vranken, J.H., *Mechanisms and Treatment of Neuropathic Pain.* Central Nervous System Agents in Medicinal Chemistry, 2009. **9**: p. 71-78.
46. Teng, J. and N. Mekhail, *Neuropathic Pain: Mechanisms and Treatment Options.* Pain Practice, 2003. **3**(1): p. 8-21.
47. Vranken, J.H., *Mechanisms and treatment of neuropathic pain.* Cent Nerv Syst Agents Med Chem, 2009. **9**(1): p. 71-8.
48. Raja, S.N. and J.A. Haythornthwaite, *Combination therapy for neuropathic pain--which drugs, which combination, which patients?* N Engl J Med, 2005. **352**(13): p. 1373-5.
49. Attal, N., et al., *EFNS guidelines on the pharmacological treatment of neuropathic pain: 2010 revision.* Eur J Neurol, 2010. **17**(9): p. 1113-e88.
50. Finnerup, N.B., S.H. Sindrup, and T.S. Jensen, *The evidence for pharmacological treatment of neuropathic pain.* Pain, 2010. **150**(3): p. 573-81.
51. Dworkin, R.H., et al., *Pharmacologic management of neuropathic pain: evidence-based recommendations.* Pain, 2007. **132**(3): p. 237-51.
52. Dworkin, R.H., et al., *Recommendations for the pharmacological management of neuropathic pain: an overview and literature update.* Mayo Clin Proc, 2010. **85**(3 Suppl): p. S3-14.
53. Merrifield, R.B., J. Am. Chem. Soc, 1963(85): p. 2149-2154.
54. Wütrich, K., ed. *NMR of proteins and nucleic acids*. 1986: New York: Wiley-Interscience.
55. Wishart, D.S., et al., *1H, 13C and 15N random coil NMR chemical shifts of the common amino acids. I. Investigations of nearest-neighbor effects.* J Biomol NMR, 1995. **5**(1): p. 67-81.
56. Edelhoch, H., *Spectroscopic determination of tryptophan and tyrosine in proteins.* Biochemistry, 1967. **6**(7): p. 1948-54.
57. Pace, C.N., et al., *How to measure and predict the molar absorption coefficient of a protein.* Protein Sci, 1995. **4**(11): p. 2411-23.

58. Halai, R., et al., *Scanning mutagenesis of alpha-conotoxin Vc1.1 reveals residues crucial for activity at the alpha9alpha10 nicotinic acetylcholine receptor.* J Biol Chem, 2009. **284**(30): p. 20275-84.
59. Vincler, M., et al., *Molecular mechanism for analgesia involving specific antagonism of alpha9alpha10 nicotinic acetylcholine receptors.* Proc Natl Acad Sci U S A, 2006. **103**(47): p. 17880-4.
60. Ellison, M., et al., *Alpha-RgIA, a novel conotoxin that blocks the alpha9alpha10 nAChR: structure and identification of key receptor-binding residues.* J Mol Biol, 2008. **377**(4): p. 1216-27.
61. McIntosh, J.M., et al., *A novel alpha-conotoxin, PeIA, cloned from Conus pergrandis, discriminates between rat alpha9alpha10 and alpha7 nicotinic cholinergic receptors.* J Biol Chem, 2005. **280**(34): p. 30107-12.
62. Nevin, S.T., et al., *Are alpha9alpha10 nicotinic acetylcholine receptors a pain target for alpha-conotoxins?* Mol Pharmacol, 2007. **72**(6): p. 1406-10.
63. Dutertre, S., A. Nicke, and R.J. Lewis, *Beta2 subunit contribution to 4/7 alpha-conotoxin binding to the nicotinic acetylcholine receptor.* J Biol Chem, 2005. **280**(34): p. 30460-8.
64. Luo, S., et al., *alpha-conotoxin AuIB selectively blocks alpha3 beta4 nicotinic acetylcholine receptors and nicotine-evoked norepinephrine release.* J Neurosci, 1998. **18**(21): p. 8571-9.
65. Clark, R.J., et al., *The synthesis, structural characterization, and receptor specificity of the alpha-conotoxin Vc1.1.* J Biol Chem, 2006. **281**(32): p. 23254-63.
66. Safavi-Hemami, H., et al., *Embryonic toxin expression in the cone snail conus victoriae - primed to kill or divergent function?* J Biol Chem, 2011.
67. Kaas, Q., et al., *ConoServer, a database for conopeptide sequences and structures.* Bioinformatics, 2008. **24**(3): p. 445-6.
68. Sarin, V.K., et al., *Quantitative monitoring of solid-phase peptide synthesis by the ninhydrin reaction.* Anal Biochem, 1981. **117**(1): p. 147-57.